siveness. *Am J Physiol* 1993; **264**: C1367–C1387.
6. Blaustein MP: Endogenous ouabain: role in the pathogenesis of hypertension. *Kidney Int* 1996; **49**: 1748–1753.
7. Nelson LD, Unlap MT, Lewis JL, Bell PD: Renal arteriolar Na^+/Ca^{2+} exchange in salt-sensitive hypertension. *Am J Physiol* 1999; **276**: F567–F573.
8. Nelson LD, Mashburn NA, Bell PD: Altered sodium-calcium exchange in afferent arterioles of the spontaneously hypertensive rat. *Kidney Int* 1996; **50**: 1889–1896.
9. Unlap MT, Peti-Peterdi J, Bell PD: Cloning of mesangial cell Na^+/Ca^{2+} exchangers from Dahl/Rapp salt-sensitive/resistant rats. *Am J Physiol Renal Physiol* 2000; **279**: F177–F184.
10. Ashida T, Kuramochi M, Omae T: Increased sodium-calcium exchange in arterial smooth muscle of spontaneously hypertensive rats. *Hypertension* 1989; **13**: 890–895.
11. Ashida T, Kawano Y, Yoshimi H, Kuramochi M, Omae T: Effects of dietary salt on sodium-calcium exchange and ATP-driven calcium pump in arterial smooth muscle of Dahl rats. *J Hypertens* 1992; **10**: 1335–1341.
12. Kraev A, Chumakov I, Carafoli E: The organization of the human gene *NCX1* encoding the sodium-calcium exchanger. *Genomics* 1996; **37**: 105–112.
13. Kofuji P, Lederer WJ, Schulze DH: Mutually exclusive and cassette exons underlie alternatively spliced isoforms of the Na/Ca exchanger. *J Biol Chem* 1994; **269**: 5145–5149.
14. Barnes KV, Cheng G, Dawson MM, Menick DR: Cloning of cardiac, kidney, and brain promoters of the feline *NCX1* gene. *J Biol Chem* 1997; **272**: 11510–11517.
15. Lee SL, Yu AS, Lytton J: Tissue-specific expression of Na^+-Ca^{2+} exchanger isoforms. *J Biol Chem* 1994; **269**: 14849–14852.
16. Nicholas SB, Yang W, Lee SL, Zhu H, Philipson KD, Lytton J: Alternative promoters and cardiac muscle cell-specific expression of the Na^+/Ca^{2+} exchanger gene. *Am J Physiol* 1998; **274**: H217–H232.
17. Scheller T, Kraev A, Skinner S, Carafoli E: Cloning of the multipartite promoter of the sodium-calcium exchanger gene *NCX1* and characterization of its activity in vascular smooth muscle cells. *J Biol Chem* 1998; **273**: 7643–7649.
18. Joint National Committee on Prevention, Detection, Evaluation, and Treatment of High Blood Pressure: The sixth report of the Joint National Committee on Prevention, Detection, Evaluation, and Treatment of High Blood Pressure. *Arch Intern Med* 1997; **157**: 2413–2446.
19. Kamide K, Tanaka C, Takiuchi S, *et al*: Six missense mutations of the epithelial sodium channel β and γ subunits in Japanese hypertensives. *Hypertens Res* 2004; 333–338.
20. Tanaka C, Kamide K, Takiuchi S, *et al*: An alternative fast and convenient genotyping method for the screening of angiotensin converting enzyme gene polymorphisms. *Hypertens Res* 2003; **26**: 301–306.
21. Inamoto N, Katsuya T, Kokubo Y, *et al*: Association of methylenetetrahydrofolate reductase gene polymorphism with carotid atherosclerosis depending on smoking status in a Japanese general population. *Stroke* 2003; **34**: 1628–1633.
22. Hwang EF, Williams I, Kovacs G, *et al*: Impaired ability of the Na^+/Ca^{2+} exchanger from the Dahl/Rapp salt-sensitive rat to regulate cytosolic calcium. *Am J Physiol Renal Physiol* 2003; **284**: F1023–F1031.
23. Meade TW, Imeson JD, Gordon D, Peart WS: The epidemiology of plasma renin. *Clin Sci* (*Lond*) 1983; **64**: 273–280.
24. Alderman MH, Madhavan S, Cohen H, Sealey JE, Laragh JH: Low urinary sodium is associated with greater risk of myocardial infarction among treated hypertensive men. *Hypertension* 1995; **25**: 1144–1152.
25. Furman I, Cook O, Kasir J, Low W, Rahamimoff H: The putative amino-terminal signal peptide of the cloned rat brain Na^+-Ca^{2+} exchanger gene (RBE-1) is not mandatory for functional expression. *J Biol Chem* 1995; **270**: 19120–19127.
26. Loo TW, Ho C, Clarke DM: Expression of a functionally active human renal sodium-calcium exchanger lacking a signal sequence. *J Biol Chem* 1995; **270**: 19345–19350.

Role of Calcineurin B Homologous Protein in pH Regulation by the Na^+/H^+ Exchanger 1: Tightly Bound Ca^{2+} Ions as Important Structural Elements†

Tianxiang Pang,‡ Takashi Hisamitsu,‡ Hidezo Mori,⊥ Munekazu Shigekawa,§ and Shigeo Wakabayashi*,‡

‡*Department of Molecular Physiology and Department of Cardiac Physiology, National Cardiovascular Center Research Institute, Suita, Osaka 565-8565, Japan, and Department of Human Life Sciences, Senri Kinran University, Suita, Osaka 565-0873, Japan*

Received November 10, 2003; Revised Manuscript Received January 27, 2004

ABSTRACT: We studied the role of the interaction of calcineurin homologous protein 1 (CHP1) with the Na^+/H^+ exchanger 1 (NHE1), particularly its EF-hand Ca^{2+} binding motifs, in the intracellular pH (pH_i)-dependent regulation of NHE1. We found that $^{45}Ca^{2+}$ binds to two EF-hand motifs (EF3 and 4) of the recombinant CHP1 proteins with high affinity (apparent K_d = ~90 nM). Complex formation between CHP1 and the CHP1 binding domain of NHE1 resulted in a marked increase in the Ca^{2+} binding affinity (K_d = ~2 nM) by promoting a conformational change of the EF-hands toward the tightly Ca^{2+}-bound form. This suggests that CHP1 always contains two Ca^{2+} ions when associated with NHE1 in cells. Interestingly, overexpression of GFP-tagged CHP1 with mutations in EF3 or EF4 significantly reduced the exchange activity in the neutral pH_i range and partly impaired the activation of NHE1 in response to various stimuli, such as growth factors and osmotic stress. Furthermore, we found that, in addition to reducing the activity (V_{max}), a CHP1 binding-defective NHE1 mutant had a marked reduction in pH_i sensitivity (~0.7 pH unit acidic shift), which consequently abolished various regulatory responses of NHE1. These observations suggest that the association of NHE1 with CHP1 is crucial for maintenance of the pH_i sensitivity of NHE1 and that tightly bound Ca^{2+} ions may serve as important structural elements in the "pH_i sensor" of NHE1.

The Na^+/H^+ exchanger (NHE1[1]) proteins in the plasma membrane and various organellar compartments of mammalian cells catalyze the electroneutral countertransport of Na^+ for H^+. Nine distinct isoforms of the Na^+/H^+ exchanger (NHE1 to NHE9) have been isolated to date, and these molecules have been shown to exhibit similar membrane topologies with 12 predicted N-terminal membrane-spanning helices and a large C-terminal cytoplasmic region (*1*−*10*). They show considerable differences in their tissue expression patterns, membrane localization, and kinetic and pharmacological properties. The plasma membrane exchangers (NHE1−5) are primarily involved in regulation of intracellular pH and Na^+ concentration, but they also participate in a broad range of physiological processes, such as cell volume regulation, transepithelial transport of electrolytes, cell proliferation, apoptosis, and differentiation (*1*−*3*).

Of the nine isoforms identified to date, NHE1 has been characterized in the most detail. NHE1 is ubiquitously expressed in essentially all tissues and cell types and plays a major role in maintaining intracellular pH and cell volume homoeostasis. The activity of NHE1 is controlled by various extrinsic factors, including growth factors, hormones, and mechanical stimuli (*1*−*3*). A variety of signaling molecules regulate the NHE1 protein, such as calcinuerin B homologous protein (CHP) (*11*−*13*), Ca^{2+}/calmodulin (*14*, *15*), the low molecular weight GTPases Ras and Rho (*16*), p42/44 mitogen-activated protein kinases (*17*), p90 ribosomal S6 kinase (*18*), 14-3-3 protein (*19*), Nck-interacting kinase (*20*), phosphatidylinositol 4,5-bisphosphate (*21*), and carbonic anhydrase II (*22*). Recently, we have focused on the role of CHP in regulation of the activities of the Na^+/H^+ exchangers (*12*, *13*).

CHP was initially discovered as a protein (p22) involved in vesicular transport (*23*), as well as a molecule that interacted with NHE (*11*). Since then, CHP has been reported

† This work was supported by Grant-in-Aid for Priority Areas 13142210 and Grant-in-Aid 14580664 for Scientific Research from the Ministry of Education, Science, and Culture of Japan, by the promotion of Fundamental Studies in Health Science of the Organization for Pharmaceutical Safety and Research of Japan (Promotion of Fundamental Studies in Health Science), and by Grant nano-001 for Research on Advanced Medical Technology from the Ministry of Health, Labor, and Welfare of Japan. T.P. was supported by a Japan Society for the Promotion of Science Postdoctoral Fellowship.

* To whom correspondence should be addressed. Department of Molecular Physiology, National Cardiovascular Center Research Institute, Fujishirodai 5-7-1, Suita, Osaka 565-8565 Japan. Tel: +81-6-6833-5012. Fax: +81-6-6835-5314. E-mail: wak@ri.ncvc.go.jp.

‡ Department of Molecular Physiology, National Cardiovascular Center Research Institute.

⊥ Department of Cardiac Physiology, National Cardiovascular Center Research Institute.

§ Senri Kinran University.

[1] Abbreviations: NHE, Na^+/H^+ exchanger; CHP, calcineurin B homologous protein; GFP, green fluorescent protein; CaN, calcineurin; CaM, calmodulin; pH_i, intracellular pH; EIPA, 5-(*N*-ethyl-*N*-isopropyl)-amiloride; DMEM, Dulbecco's modified Eagle's medium; HEPES, 2-[4-(2-hydroxyethyl)-1-piperazinyl]ethansulfonic acid; Tris, Tris(hydroxymethyl)aminomethane; EGTA, *O*,*O*′-bis(2-aminoethyl)ethylene glycol-*N*,*N*,*N*′,*N*′-tetraacetic acid; PBS, phosphate-buffered saline; PDGF-BB, platelet-derived growth factor-BB; PMA, phorbol 12-myristate 13-acetate; SDS−PAGE, sodium dodecyl sulfate−polyacrilamide gel electrophoresis.

10.1021/bi0360004 CCC: $27.50
Published on Web 03/06/2004

to exhibit multiple functions, including inhibition of calcinuerin phosphatase activity (*24*), as well as interaction with microtubules (*25*), DRAK2 (death-associated protein kinase related apoptosis inducing protein kinase 2) (*26*) and KIF1Bβ2 (kinesin-family 1Bβ2) (*27*). Previously, we reported that the ubiquitous CHP isoform (designated as CHP1) is an essential cofactor for the physiological activity of the Na^+/H^+ exchanger by interacting with the juxtamembrane region in the C-terminal cytoplasmic domain of plasma membrane exchanger isoforms (*12*). Furthermore, we reported that the second CHP isoform (CHP2) might be involved in maintenance of the abnormally high pH_i in malignantly transformed cells (*13*). CHP2 is expressed at a relatively high level in the rat small intestine (*28*), suggesting that it plays a specific role in this tissue. These CHP proteins contain four EF-hand Ca^{2+} binding motifs and are myristoylated at the N-terminus (Gly^2). In addition, CHP1 is phosphorylated in cells in a serum-dependent manner (*11*). However, the roles of these posttranslational modifications of CHP proteins in the pH_i-dependent regulation or acute activation of NHE in response to extracellular stimuli are largely unknown, although this protein family appears to be essential for the physiological exchange activity of plasma membrane NHEs.

In this study, we focused on the EF-hand Ca^{2+} binding motifs of CHP1. We found that the affinity of CHP1 for Ca^{2+} markedly (approximately 40-fold) increases upon complex formation with NHE1, probably by promoting a change in the conformation of the EF-hand motifs. The extremely low Ca^{2+} dissociation constant (~2 nM) of CHP1 suggests that Ca^{2+} ions remain tightly bound to CHP1 when it is complexed with NHE1 in the plasma membrane. On the basis of properties of various CHP1 and NHE1 mutant proteins in cells, we suggest that CHP1 is important for pH_i-dependent regulation of NHE1 and that tightly bound Ca^{2+} ions play an important role in maintaining a structure that is critical for this function of CHP1.

EXPERIMENTAL PROCEDURES

Materials. The amiloride derivative EIPA was a gift from the New Drug Research Laboratories of Kanebo, Ltd. (Osaka, Japan). $^{45}CaCl_2$, $^{22}NaCl$, and ^{14}C-benzoic acid were purchased from Dupont-NEN (Boston, MA). The rabbit polyclonal antibodies against CHP1 and NHE1 were described previously (*12*, *14*). All other chemicals were of the highest purity available.

Cells, Culture Conditions, and Stable Expression. The exchanger-deficient cell line PS120 (*29*) and corresponding transfectants were maintained in DMEM (Life Technologies Inc., Rockville, MD) containing 25 mM $NaHCO_3$ and supplemented with 7.5% (v/v) fetal calf serum, penicillin (50 units/mL), and streptomycin (50 μg/mL). Cells were maintained at 37 °C in the presence of 5% CO_2. PS120 cells (5×10^5 cells/100-mm dish) were transfected with each plasmid construct (20 μg) by the calcium phosphate coprecipitation technique. Cell populations stably expressing wild-type or mutant human NHE1 were selected by the H^+-killing procedure as described previously (*30*). Cells stably overexpressing GFP-tagged CHP1 were first selected with G418, and then single colonies were selected by monitoring GFP fluorescence.

Construction of Expression Vectors. All the constructs were produced by means of a polymerase chain reaction (PCR)-based strategy. For construction of GFP-tagged CHP1 or its mutant forms with mutations in Ca^{2+} binding motifs or in the myristoylated glycine (G2A), a cDNA encoding CHP1 was cloned into the mammalian expression vector pEGFP-N1 (Clontech, Palo Alto, CA). The plasmids carrying cDNAs for the wild-type or mutant NHE1s were all cloned into the mammalian expression vector pECE. Constructs were confirmed by sequencing plasmids with an ABI-PRISM DNA sequencer model 3100 (Applied Biosystems, Foster City, CA).

Purification of Recombinant Proteins. Recombinant histidine-tagged CHP1 proteins were produced in *Escherichia coli* (BL21-Star; Invitrogen, San Diego, CA) transformed with pET11 carrying the cDNA encoding CHP1 containing the C-terminal six histidine residues as described previously (*12*). Myristoylated CHP1 was produced using the same bacteria except they also contained the vector pBB131, which carries the yeast *N*-myristoyltransferase cDNA (kindly provided by Dr. J. I. Gordon, Washington University). Myristoylation of CHP1 (or p22) produced by this method was previously confirmed (*23*). For production of the complex of CHP1 and the CHP1 binding region of NHE1, the cytoplasmic region (aa 503−545) of NHE1 was cloned into the vector pET24 and coexpressed with His-tagged CHP1 in *E. coli* in the presence of ampicillin and kanamycin. Myristoylated and nonmyristoylated CHP1 proteins and CHP1/NHE1 (aa 503−545) complex proteins were all recovered in the soluble fraction and partially purified by passage through a Ni^{2+} affinity resin column (ProBond, Invitrogen) according to the manufacturer's protocol. Partially purified CHP1 proteins were found to be ~70% pure. We did not carry out further purification of CHP1 because of aggregation during storage. The complexes consisting of CHP1 or its mutant variants complexed with the NHE1 fragment were further purified to more than 95% by diethylaminoethyl-Sepharose column chromatography. All the proteins were dialyzed overnight against 60 mM KCl and 10 mM HEPES/Tris (pH 7.2).

Measurement of Equilibrium $^{45}Ca^{2+}$ Binding. $^{45}Ca^{2+}$ binding to the proteins was measured by a filtration method as described previously (*31*). Purified proteins (0.1−0.2 mg/mL) were incubated for 1 h at 25 °C in a solution containing 60 mM KCl, 5 mM $MgCl_2$, 50 μM $CaCl_2$, 0.02 μCi/mL $^{45}CaCl_2$, 10 mM HEPES/Tris (pH 7.2), and different concentrations of EGTA (0−58 mM), giving a free Ca^{2+} concentration of 0.1 nM to 50 μM. Aliquots (1 mL) of the reaction mixture were transferred onto 0.22-μm Millipore filters (Millipore, Bedford, MA) and filtered under vacuum. As controls, the same reaction mixtures without proteins were filtered to measure the background binding of ^{45}Ca by the filters. More than 95% of the proteins were retained in the filters. After the filters were dried, ^{45}Ca radioactivity was measured by scintillation counting.

Measurement of $^{45}Ca^{2+}$ Release from Proteins. $^{45}Ca^{2+}$ release from proteins was measured using a rapid filtration apparatus as described previously (*31*). After preincubation of proteins with a solution containing 50 μM $^{45}CaCl_2$ for 1 h, aliquots (1 mL) of reaction mixtures were filtered through Millipore filters. Filters were washed at a constant rate (0.2−2 mL/s) for the indicated periods (0.2−30 s) with

0.4−6 mL of 60 mM KCl, 5 mM $MgCl_2$, 10 mM HEPES/Tris (pH 7.2), and 10 mM EGTA. After the filters were dried, ^{45}Ca radioactivity was measured by scintilation counting.

Immunoprecipitation and Immunoblotting. Immunoprecipitation and immunoblotting were performed essentially as described previously (*14*). Briefly, cells were solubilized with 1% Triton X-100 in a solution of 150 mM NaCl, 10 mM HEPES-Tris (pH 7.4), and protease inhibitors. Cell lysates were incubated with respective antibodies and protein A Sepharose. After centrifugation, precipitated materials were separated on 7.5% or 12% polyacrylamide gels and electrophoretically transferred to Immobilon membranes (Millipore). After blocking, incubation with antibodies and washing, protein signals were visualized by enhanced chemiluminescence (Amersham, Buckinghamshire, U.K.). The signal intensity was measured using a photonic microscope system (ARUGUS-100, Hamamatsu photonics).

Measurement of $^{22}Na^+$ Uptake. $^{22}Na^+$ uptake activity and its pH_i dependence were measured by the K^+/nigericin pH_i clamp method essentially as described previously (*32*). Serum-depleted cells in 24-well dishes were incubated for 30 min at 37 °C in Na^+-free choline chloride/KCl medium containing 20 mM HEPES/Tris (pH 7.4), 1.2−140 mM KCl, 2 mM $CaCl_2$, 1 mM $MgCl_2$, 5 mM glucose (or 5 mM 2-deoxyglucose plus 2 μg/mL oligomycin under conditions of ATP depletion), and 5 μM nigericin. $^{22}Na^+$ uptake was started by adding the same choline chloride/KCl solution containing $^{22}NaCl$ (37 kBq/mL, final concentration = 1 mM), 1 mM ouabain, and 100 μM bumetanide. In some wells, 0.1 mM EIPA was added to the solution. After 1 min, cells were washed four times with ice-cold PBS to terminate $^{22}Na^+$ uptake. The pH_i was calculated from the imposed K^+ concentration gradient by assuming the equilibrium $[K^+]_i/[K^+]_o = [H^+]_o/[H^+]_i$ and an intracellular K^+ concentration of 120 mM. Data were normalized according to the protein concentration as measured by the bicinchoninic assay (Pierce Chemical Co., IL) using bovine serum albumin as a standard.

Measurement of pH_i. Changes in pH_i were measured by the [^{14}C]-benzoic acid equilibration method (*30*). For this measurement, serum-depleted cells were incubated for 30 min in bicarbonate-free HEPES-buffered DMEM (pH 7.0) and then incubated in the same medium containing [^{14}C]-benzoic acid (37 kBq/mL) for 20 min at 37 °C. After the cells were washed four times with ice-cold PBS, ^{14}C-radioactivity taken up by cells was measured. Changes in pH_i were calculated as described previously (*30*).

Statistics. Data of the pH dependence of EIPA-sensitive $^{22}Na^+$ uptake were simulated by fitting the values to the sigmoidal dose-response equation, rate of EIPA-sensitive $^{22}Na^+$ uptake = $V_{max}/(1 + 10^{\log(pK - pH_i)n})$ (pK = pH_i giving half-maximal $^{22}Na^+$ uptake; n = Hill coefficient), using the simulation program included in Graphpad Prizm (Microsoft Corp., Redmond, WA). Equilibrium $^{45}Ca^{2+}$ binding was fitted to the dose−response equation, $^{45}Ca^{2+}$ bound = maximal $^{45}Ca^{2+}$ bound/$(1 + (K_d - [Ca^{2+}])^n)$ (K_d = apparent dissociation constant for Ca^{2+}; n = Hill coefficient). Kinetic parameters were expressed as the best fit values with standard errors, whereas other data were expressed as the means ± SD for at least three determinations.

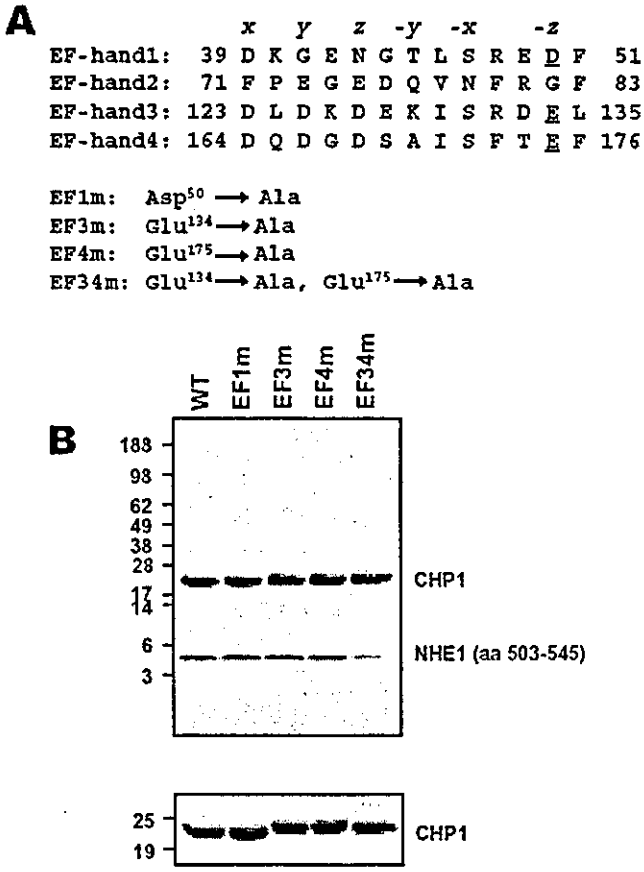

FIGURE 1: Amino acid sequences of EF-hand motifs and purified proteins of various CHP1 mutants. Panel A shows amino acid sequences of four EF-hand motifs present in CHP1. In four mutant CHP1s (EF1m, EF3m, EF4m, and EF34m), Asp^{50}, Glu^{134}, Glu^{175}, and both Glu^{134}/Glu^{175} were replaced by alanine. In panel B, the purified complex of His-tagged CHP1 with the NHE1 segment (aa 503−545) (10 μg) was separated by electrophoresis on a 4−15% gradient (upper panel) or 12% SDS−PAGE gel (lower panel) and then visualized by Coomassie Brilliant Blue staining.

RESULTS

Characterization of Ca^{2+} Binding Motifs in CHP1. We first analyzed $^{45}Ca^{2+}$ binding to EF-hand motifs of CHP1 using recombinant CHP1 and its complex with the binding domain in NHE1. CHP1 interacts with NHE1 at the juxtamembrane region of the carboxyl-terminal cytoplasmic domain of NHE1. Hydrophobic residues of NHE1, such as Phe^{526}, Leu^{527}, Leu^{530}, and Leu^{531}, were shown to be important for the interaction of CHP1 with NHE1 (*12*). CHP1 contains four potential EF-hand Ca^{2+} binding motifs, of which two ancestral sites (EF1 and -2) may not bind Ca^{2+} due to substitution of critical acidic residues (Figure 1A). The canonical EF-hand consists of 29 consecutive residues with two flanking helices and a 12-residue loop (Figure 1A). The chelating loop residues in positions 1 (+x), 3 (+y), 5 (+z), 7 (−y), 9 (−x), and 12 (−z) ligate Ca^{2+} through seven oxygen atoms arranged three-dimensionally on the axes of a pentagonal bipyramid (*33*, *34*). The −z position, providing the only side chain oxygen atoms, is crucial for Ca^{2+} binding (*33*−*35*). To characterize these Ca^{2+} binding motifs, we introduced mutations into EF1, -3, and -4 in which acidic residues (aspartic acid or glutamic acid) at the −z position were replaced by alanine (Figure 1B). We coexpressed the wild-type or mutant CHP1s together with the juxtamembrane region of NHE1 (aa 503−545) in *E. coli*. We confirmed that

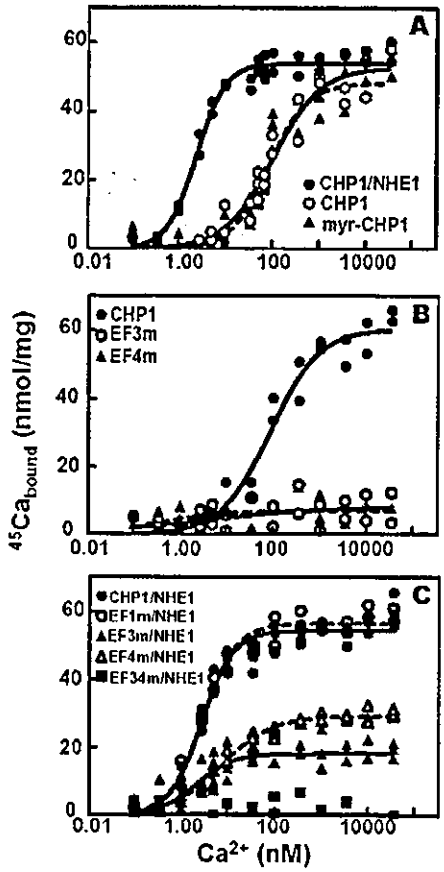

FIGURE 2: Equilibrium $^{45}Ca^{2+}$ binding to various CHP1 mutant proteins. In panels A–C, CHP1 or its various mutant proteins and the complex of CHP1 variants with the NHE1 segment (aa 503–545) (0.1–0.2 mg/mL) were incubated for 1 h in solutions containing 50 μM $^{45}CaCl_2$ and various concentrations of EGTA, which produce 0.2 nM to 50 μM free Ca^{2+}. Symbols corresponding to each protein variant were indicated in figures. The solutions were filtered through Millipore filters, and $^{45}Ca^{2+}$ bound to the CHP1 proteins was measured.

the purified complex proteins (>95% pure) of the wild-type CHP1, EF1m, EF3m, or EF4m with aa 503–545 of NHE1 were retained as a single peak on gel filtration chromatography and contained the CHP1 variant and the NHE1 peptide at a 1:1 molar ratio (data not shown). In addition, using 4–15% polyacrylamide gradient gels, we confirmed that the purified samples mostly contained comparable molar amounts of the CHP1 variant and the NHE1 fragment (Figure 1B, upper panel). However, in EF34m with double mutations at EF3 and -4, the amount of the NHE1 fragment was significantly reduced, suggesting that this double mutation impairs the interaction of CHP1 with NHE1. On 12% SDS–PAGE, EF3m, EF4m, and EF34m proteins were found to migrate more slowly than the wild-type or EF1m proteins (Figure 1B, lower panel), suggesting that a mutation-induced conformational change occurred in these three mutant proteins that had impaired Ca^{2+} binding (see below).

We measured $^{45}Ca^{2+}$ binding to various CHP1 mutant proteins by a membrane filtration procedure. We found that $^{45}Ca^{2+}$ bound to the partially purified CHP1 proteins with an apparent K_d of ~90 nM (Figure 2A and Table 1). The maximal amount of $^{45}Ca^{2+}$ bound to CHP1 corresponded to ~2 mol of Ca^{2+} bound/mol of CHP1, assuming that the CHP1 sample was 70% pure. Myristoylation did not significantly affect the apparent affinity for Ca^{2+} nor the

Table 1: Parameters for Equilibrium $^{45}Ca^{2+}$ Binding

proteins	apparent K_d ± SE (nM)[a]	Hill coefficient ± SE
CHP1	89.9 ± 9.3	0.77 ± 0.12
myr-CHP1	86.4 ± 8.9	0.94 ± 0.17
CHP1/NHE1	2.32 ± 0.18	1.22 ± 0.15
EF1m/NHE1	2.17 ± 0.39	0.98 ± 0.14
EF3m/NHE1	2.89 ± 0.28	1.27 ± 0.55
EF4m/NHE1	2.24 ± 0.26	0.76 ± 0.09

[a] The data shown in Figure 2 were fitted to the equation for equilibrium $^{45}Ca^{2+}$ binding as described in Experimental Procedures.

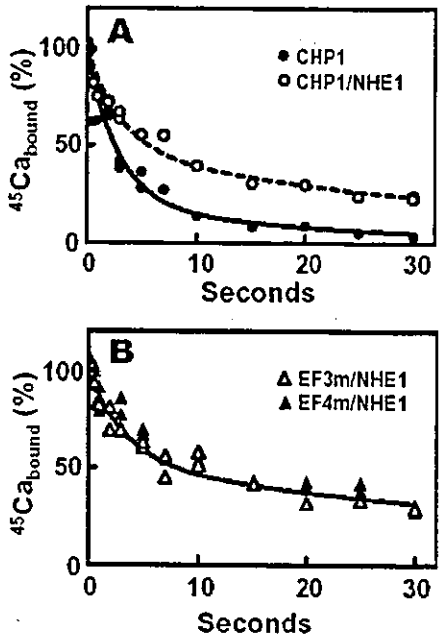

FIGURE 3: Time courses of $^{45}Ca^{2+}$ release from CHP1 proteins: (A) $^{45}Ca^{2+}$ release from CHP1 alone (●) or CHP1/NHE1 complex (○); (B) $^{45}Ca^{2+}$ release from EF3m/NHE1 (△) or EF4m/NHE1 complex (▲). CHP1 proteins or the complex of CHP1 variants with the NHE1 segment (aa 503–545) (0.1–0.2 mg/mL) were incubated for 1 h in a solution containing 50 μM $^{45}CaCl_2$, applied to Millipore filters, and washed with a solution containing EGTA. $^{45}Ca^{2+}$ remaining on the filters was measured.

maximal level of $^{45}Ca^{2+}$ binding (Figure 2A and Table 1). Interestingly, when CHP1 formed a complex with the NHE1 fragment, the binding affinity for $^{45}Ca^{2+}$ increased markedly (~40-fold, Figure 2A and Table 1). The extremely low apparent dissociation constant (~2 nM) deviates substantially from the physiological cytosolic Ca^{2+} concentration of cells (0.1–10 μM). The maximal level of Ca^{2+} binding on the complex again corresponded to ~2 mol of Ca^{2+} bound/mol of CHP1. Mutation of either of Ca^{2+} binding motifs EF3 or EF4, but not EF1, resulted in loss of approximately 1 mol of $^{45}Ca^{2+}$ bound to the complex (Figure 2C). On the other hand, $^{45}Ca^{2+}$ binding was completely blocked when the experiment was carried out using EF3m and EF4m proteins but without the NHE1 fragment (Figure 2B) or when two sites were simultaneously mutated (EF34m) (Figure 2C). Together, these results indicate that CHP1 binds two Ca^{2+} ions, one at EF3 and the other at EF4.

To determine how complex formation increases the Ca^{2+} binding affinity, we measured $^{45}Ca^{2+}$ release from CHP1 proteins by rapid filtration. As shown in Figure 3A, most of the $^{45}Ca^{2+}$ bound to CHP1 without the NHE1 fragment was released rapidly ($t_{1/2}$ = ~2 s). In contrast, $^{45}Ca^{2+}$ release from

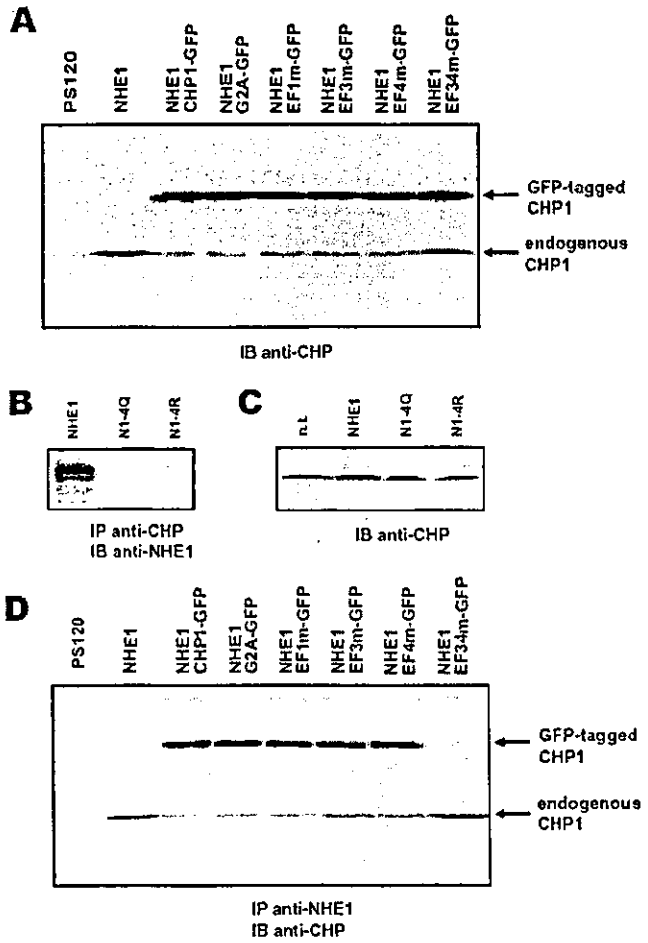

FIGURE 4: Expression of various GFP-tagged CHP1 proteins and their coimmunoprecipitation with NHE1. Panel A shows the expression level of GFP-tagged CHP1 and its variants (indicated at the top of the figure). Cell lysates (50 μg) from stable transfectants were subjected to SDS–PAGE, and expression of endogenous and exogenous CHP1 proteins were detected by immunoblotting (IB) with an anti-CHP1 antibody. A result for untransfected PS120 cells is shown in the first lane. Panel B shows coimmunoprecipitation of the wild-type or mutant (4Q and 4R) exchangers with endogenous CHP1. Lysates from cells stably expressing these exchangers were subjected to immunoprecipitation with anti-CHP1 antibody followed by immunoblotting with anti-NHE1 antibody. Panel C shows the expression level of endogenous CHP1 in cells expressing the wild-type or mutant NHE1s: n.t., no transfection. Panel D shows coimmunoprecipitation of CHP1 proteins with NHE1. Lysates from cells stably expressing various proteins were subjected to immunoprecipitation with anti-NHE1 antibody followed by immunoblotting with anti-CHP1 antibody. Note that in lanes from cells not transfected with GFP-tagged CHP1 (left two lanes), IgG protein bands were visible at the same positions as GFP-tagged CHP1.

CHP1 complexed with the NHE1 fragment ($t_{1/2}$ = ~7 s) was much slower. A slow release of $^{45}Ca^{2+}$ also occurred in two mutant CHP1 proteins, EF3m and EF4m, complexed with the NHE1 fragment (Figure 3B), suggesting that Ca^{2+} binds tightly to each EF hand.

Effects of CHP1 Mutations on NHE1 Regulation. To study the role of Ca^{2+} binding in NHE1 regulation by CHP1, we transfected GFP-tagged CHP1 into cells expressing NHE1 and obtained cells stably coexpressing these proteins. The results indicated that GFP-tagged CHP1 and its mutant derivatives were highly coexpressed in NHE1 transfectants (Figure 4A). Interestingly, expression of NHE1 markedly increased the level of expression of the endogenous CHP1 (3.6-fold), while coexpression of various GFP-tagged CHP1 variants, with the exception of CHP1-EF34m-GFP, reduced it (Table 2).

Table 2: Relative Amounts of Expressed GFP-Tagged CHP1 and Endogenous CHP1

transfected proteins	relative amount of GFP-tagged CHP1[a]	relative amount of endogenous CHP[b]
untransfected		1.00 ± 0.08
NHE1		3.63 ± 0.81[c]
NHE1 + CHP1-GFP	1.00 ± 0.11	1.11 ± 0.13
NHE1 + G2A-GFP	1.08 ± 0.11	1.03 ± 0.16
NHE1 + EF1m-GFP	0.93 ± 0.06	1.07 ± 0.11
NHE1 + EF3m-GFP	0.97 ± 0.11	1.15 ± 0.16
NHE1 + EF4m-GFP	1.06 ± 0.07	1.09 ± 0.10
NHE1 + EF34m-GFP	0.94 ± 0.12	3.85 ± 0.45[c]
NHE1-4Q		1.02 ± 0.09
NHE1-4R		1.03 ± 0.06

[a] The density of visualized protein bands on immunoblots (cf. Figure 4, panels A and C) is represented as values normalized according to the band density from cells expressing CHP1-GFP. Data are means ± SD (n = 3). [b] The band density is represented as values normalized according that from untransfected PS120 cells. Data are means ± SD (n = 3). [c] $P < 0.05$ versus control.

We further examined the effect of expression of CHP1 binding-defective NHE1 mutants 4Q and 4R on the amount of endogenous CHP. These mutant exchangers do not bind CHP1 as shown by coimmunoprecipitation studies (Figure 4B). The level of expression of the endogenous CHP1 did not increase on coexpression of these mutant exchangers (Figure 4B,C, Table 2). Thus, the amount of endogenous CHP1 in cells is highly dependent on expression of NHE1 and GFP-tagged CHP1.

Figure 4D shows the results for coimmunoprecipitation experiments using NHE1- and CHP1-specific antibodies to determine interactions of the expressed CHP1–GFP with NHE1. Anti-NHE1 antibody immunoprecipitated endogenous CHP1 from cells expressing NHE1. In cells coexpressing GFP–CHP1 and NHE1, the same antibody coimmunoprecipitated large quantities of GFP–CHP1 or its derivatives, and at the same time, the amount of immunoprecipitated endogenous CHP1 was markedly reduced. In cells coexpressing EF34m–GFP and NHE1, anti-NHE1 antibody coimmunoprecipitated the endogenous CHP1 but not exogenous GFP-tagged mutant CHP1, consistent with the findings of in vitro binding studies indicating that double mutation at EF3 and EF4 impairs the interaction of CHP1 with NHE1.

We next examined the subcellular localization of GFP-tagged CHP1. As reported previously (*12*), the GFP-tagged CHP1 is localized in the plasma membrane in cells coexpressing NHE1 (Figure 5A). Consistent with the in vitro binding data (Figure 1B), the GFP fluorescence was observed in the plasma membrane in cells coexpressing GFP-tagged CHP1 mutants except EF34m with NHE1 (Figure 5A; data not shown for G2A and EF1m). These results, together with the data from coimmunoprecipitation experiments, indicate that the endogenous CHP1 bound to NHE1 was efficiently replaced by expressed GFP-tagged wild-type or CHP1 mutants. However, the double mutant EF34m was not localized at the plasma membrane (Figure 5A) because of the weak interaction of this mutant protein with the juxtamembrane region of NHE1. We observed that GFP fluorescence was still observed in the plasma membrane after addition of phorbol ester, serum, thrombin, lysophosphatidic

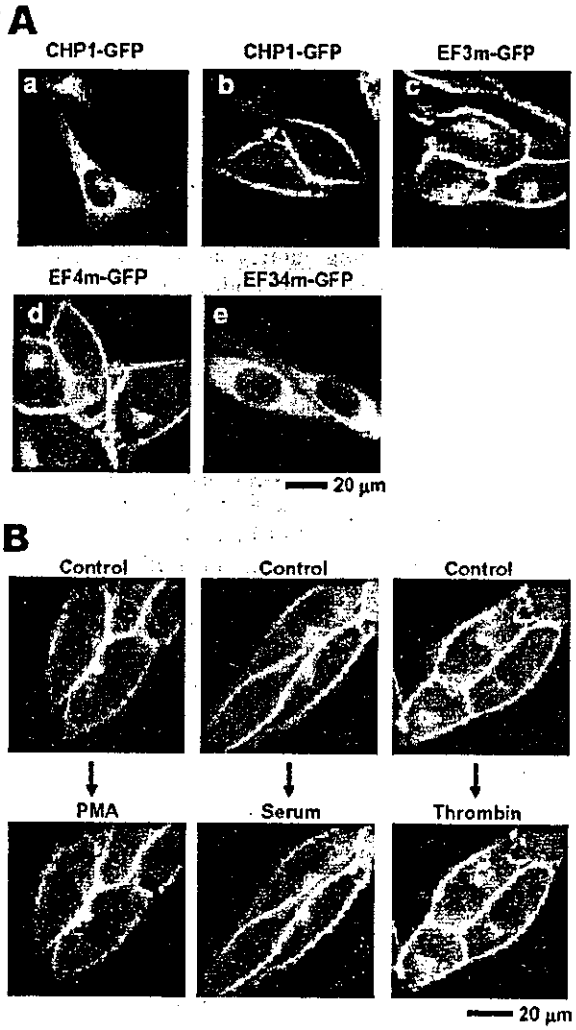

FIGURE 5: Subcellular localization of GFP-tagged CHP1: (A) subcellular localization of GFP-tagged wild-type CHP1 (a, b), EF3m (c), EF4m (d), and EF34m (e) expressed in PS120 cells (a) or in their stable transfectants of the wild-type NHE1 (b–e); (B) effect of various agents on the subcellular localization of the wild-type GFP-tagged CHP1 in NHE1 transfectants. Cells were placed in serum-free Dulbecco's modified Eagle's medium without phenol red for 5 h, and then 1 μM PMA, 10% serum, or 2 units/ml thrombin were added. GFP fluorescence was observed under a fluorescent microscope equipped with a CoolSNAP imaging system (RS Photometrics) before (control) and 20 min after addition of the various agents.

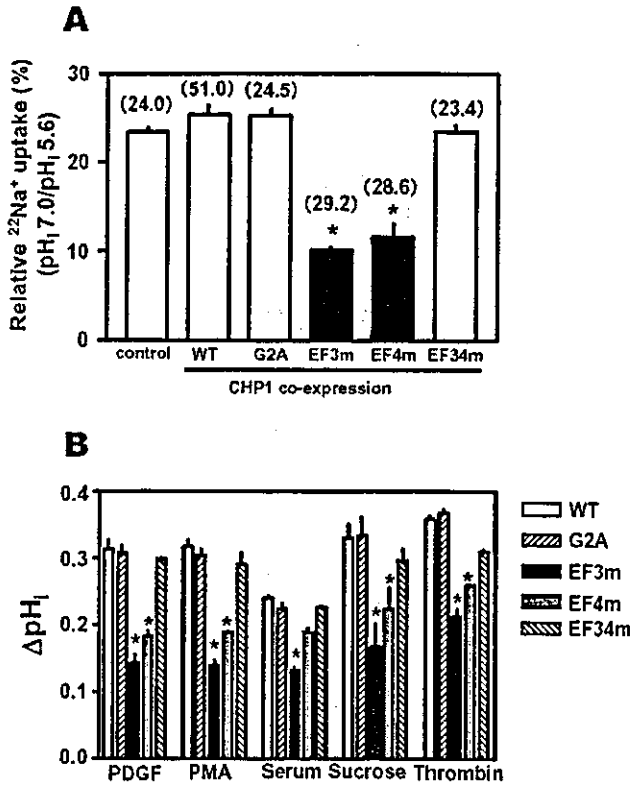

FIGURE 6: Exchange activity and regulation of NHE1 transfectants expressing various CHP1 mutants. Panel A shows ratios of EIPA-sensitive $^{22}Na^+$ uptake activities of cells coexpressing wild-type NHE1 and various CHP1 mutants at pH_i 7.0 and 5.6. Numbers (nmol/mg/min) in parentheses represent $^{22}Na^+$ uptake activity at $pH_i = 5.6$. Control cells were not transfected with CHP1 but stably expressing NHE1. Data are means ± SD ($n = 3$; *, $P < 0.05$ versus cells not expressing exogenous CHP1). Panel B shows changes in pH_i measured using the [^{14}C]benzoic acid equilibration method. The cells coexpressing NHE1 and various CHP1 variants were stimulated for 15 min at 37 °C with 10 ng/mL PDGF-BB, 1 μM PMA, 10 μg/mL lysophosphatidic acid, or 200 mM sucrose (hyperosmotic stress). Data are means ± SD ($n = 6$; *, $P < 0.05$ versus cells expressing wild-type CHP1).

acid, or PDGF-BB, which are all known to activate the exchange activity (Figure 5B, data not shown for some experiments). We also found that the plasma membrane localization of GFP fluorescence did not change upon addition of metabolic inhibitors (2-deoxyglucose plus oligomycin) that cause cell ATP depletion, thus inhibiting exchange activity (data not shown). Furthermore, we found no changes in the plasma membrane localization of GFP-tagged CHP1 mutants EF3m and EF4m after these various treatments (data not shown). These observations suggest that CHP1 is tightly associated with NHE1 in the plasma membrane and that this interaction is not affected by various stimuli.

All the cells expressing CHP1–GFP or its mutant derivatives exhibited high Na^+/H^+ exchange activity. The $^{22}Na^+$ uptake activity in cells clamped at acidic pH_i (5.6) by the K^+/nigericin technique was in the range of 20–50 nmol/mg/min (data not shown). We compared the $^{22}Na^+$ uptake activities in cells expressing various CHP1 variants in the physiological pH_i range. As shown in Figure 6A, the ratio of $^{22}Na^+$ uptake at pH_i 7.2–5.6 was not significantly altered by expression of wild-type CHP1. Although a previous study (*11*) indicated that overexpression of CHP1 inhibits the NHE1 activity in the presence of serum, we observed no such CHP1-induced inhibition of the exchange activity. The reason for this discrepancy is unknown. Unlike the wild-type CHP1, the $^{22}Na^+$ uptake ratio was significantly reduced by EF3 or EF4 mutants. Consistent with this finding, we observed that mutations of EF3 or EF4 significantly reduced the cytoplasmic alkalinization in response to PDGF-BB, thrombin, phorbol ester, serum, or hyperosmotic stress (sucrose) (Figure 6B). These observations suggest that mutation of EF3 or EF4 partly impairs the regulation of NHE1 by reducing pH_i sensitivity. In contrast, double mutation (EF34m) of CHP1 at EF3 and EF4 did not reduce the $^{22}Na^+$ uptake ratio or cytoplasmic alkalinization (Figure 6A,B), consistent with the finding that this mutant CHP1 is not able to replace the endogenous CHP1 because of its weak interaction with NHE1. Finally, mutation of the myristoylation site (G2A) or EF1 did not affect pH_i-dependent regulation of NHE1.

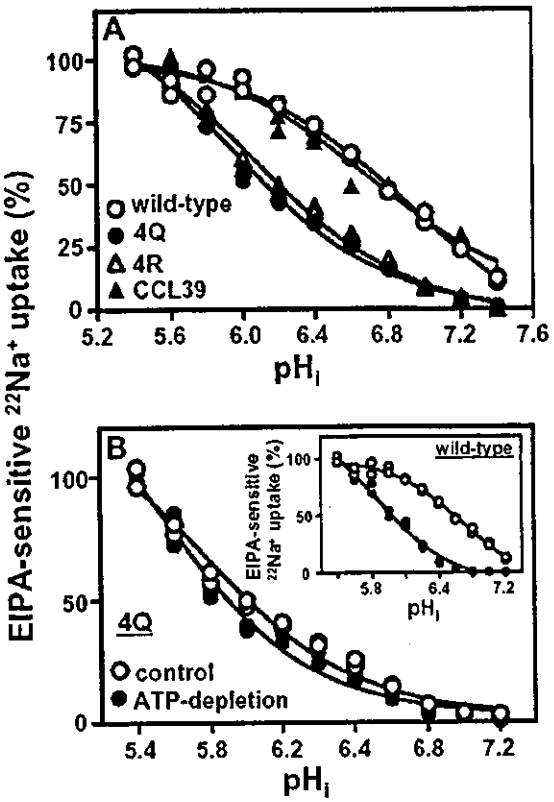

FIGURE 7: pH$_i$ dependence of exchange activity in cells expressing some NHE variants. Panel A shows the pH$_i$ dependence of ^{22}Na$^+$ uptake in PS120 cells expressing wild-type NHE1 or CHP1 binding-defective mutants 4Q and 4R and CCL39 fibroblastic cells (the parental cell line of PS120). pH$_i$ was clamped at various values with K$^+$/nigericin. The maximal EIPA-sensitive ^{22}Na$^+$ uptake activity measured at pH$_i$ = 5.4 was high in cells expressing wild-type NHE1 (~50 nmol/mg/min), while it was lower but similar in cells expressing 4Q or 4R or in CCL39 cells (4.2, 4.2, or 4.1 nmol/mg/min, respectively). Data were normalized according to the maximal activity at pH$_i$ = 5.4. Panel B shows the effects of ATP depletion on pH$_i$ dependence of exchange activity in cells expressing 4Q or wild-type NHE1 (inset). Cells were depleted of ATP by treatment with the metabolic inhibitors 2-deoxyglucose (5 mM) and oligomycin (2 μg/mL). Data were normalized according to the maximal activity at pH$_i$ = 5.4.

Properties of NHE1 Mutants Lacking CHP1 Binding. As described above, mutations of CHP1 partly impair pH$_i$-dependent regulation of NHE1. Therefore, it is of interest to determine how CHP1 binding affects the pH$_i$ sensitivity of NHE1. Previously, we described two CHP1 binding-defective mutant exchangers, 4Q or 4R, in which Phe^{526}, Leu^{527}, Leu^{530}, and Leu^{531} of NHE1 were replaced by four glutamine or arginine residues, respectively (*12*) (see Figure 4B). In this study, by using extensive H$^+$-killing selection, we obtained cells overexpressing 4Q or 4R and exhibiting relatively high activity (~4 nmol/mg/min at pH$_i$ 5.4), thus allowing reliable measurement of the pH$_i$ dependence of ^{22}Na$^+$ uptake. As shown in Figure 7A, these mutations caused a marked acidic shift in the pH$_i$ dependence (Figure 7A). As a control, we confirmed that CCL39 cells (the parental cell line of PS120) that exhibit exchange activity (V_{max}) comparable to 4Q or 4R show a pH$_i$ dependence of exchange similar to that of PS120 cells overexpressing NHE1. In cells expressing these mutant exchangers, ATP depletion did not change the pH$_i$ sensitivity of ^{22}Na$^+$ uptake (Figure 7B). In addition, cytoplasmic alkalinization in response to extracellular stimuli, such as thrombin, PDGF-BB, hyperosmolarity, LPA, and PMA, was not observed in cells expressing 4Q or 4R (data not shown), consistent with the finding that these mutants exhibit an acidic shift of pH$_i$ dependence.

DISCUSSION

In this study, we examined the role of CHP1, particularly its EF-hand Ca^{2+} binding motifs, in the pH$_i$-dependent regulation of NHE1. Our results indicated that a Ca^{2+} ion binds to each of EF3 and EF4 in CHP1 with an overall apparent K_d of ~90 nM and a Hill coefficient of ~1.0 (Table 1). This Ca^{2+} binding affinity was close to that of another family member, CaN-B (apparent $K_d \approx 70$ nM) (*36*), although the apparent K_d values for Ca^{2+} in other EF-hand Ca^{2+} binding proteins vary widely (0.01−10 μM) (*36*−*39*). Although CHP1 potentially has four Ca^{2+} binding motifs, the two ancestral sites EF1 and EF2 do not bind Ca^{2+}. This is in sharp contrast to CaN-B in which all four EF-hand motifs are able to bind Ca^{2+}, although the two N-terminal sites, EF1 and EF2, have lower affinity for Ca^{2+} than the C-terminal sites, EF3 and EF4 (*36*). Intriguingly, the Ca^{2+} affinity of CHP1 increased markedly upon complex formation with the NHE1 fragment (aa 503−545). Consistent with this finding, ^{45}Ca^{2+} release from the complex was much slower than that from CHP1 alone. The extraordinarily high affinity of CHP1 for Ca^{2+} (~2 nM) suggests that the CHP1/NHE1 complex always contains two Ca^{2+} ions under physiological conditions.

The high affinity for Ca^{2+} was also observed in mutant CHP1 proteins EF3m and EF4m, which have a single Ca^{2+} binding site, complexed with the NHE1 fragment. Increases in the affinity for Ca^{2+} by interaction with target proteins have also been reported for other Ca^{2+} binding proteins. For example, the Ca^{2+} binding affinity for calmodulin was increased 16- to 38-fold upon interaction with myosin light chain kinase (*40*), 2.6-fold with myristoylated alanine-rich protein kinase C substrate peptide (*41*), and 75-fold with the calmodulin binding peptide in CaN-A (*36*). CHP1 was reported to interact with other proteins, such as microtubules (*25*), CaN-A (*24*), DRAK2 (*26*), and KIF1Bβ2 (*27*), as well as members of the NHE1 family. Therefore, interaction with these proteins may also modify the Ca^{2+} binding affinity of CHP1.

Although mutation of CHP1 at either EF3 or EF4 impaired binding of 1 mol of Ca^{2+}, it did not appear to affect the interaction of CHP1 with NHE1 as shown by in vitro binding of these mutant proteins, coimmunoprecipitation, and the plasma membrane localization of GFP-tagged CHP1. Therefore, these mutations do not appear to induce marked structural distortions. However, double mutation (EF34m) at both EF3 and EF4 impaired the interaction of CHP1 with NHE1. Consistent with this finding, Ca^{2+} removal by EGTA from the wild-type CHP1 reduced the interaction with NHE1 in a pull-down assay through the amyrose resin column (data not shown). Thus, the tight association of NHE1 with CHP1 requires binding of at least one Ca^{2+} on either EF3 or EF4. Furthermore, it should be noted that the effect of double mutation (EF34m) on regulation of NHE1 cannot be properly analyzed in cells that express endogenous CHP1.

We found that expression of NHE1, but not the CHP1 binding-deficient mutant derivatives 4Q and 4R, significantly

increased the amount of endogenous CHP1. However, coexpression of GFP-tagged CHP1 proteins (wild-type, EF3m, and EF4m) preserving the strong interaction with NHE1 greatly reduced the amount of endogenous CHP1. Thus, the amount of endogenous CHP1 in cells is strongly dependent on the number of available CHP1 binding sites provided from NHE1. Although the precise reason for this is unknown, it is likely that interaction with target proteins is required for stable expression of CHP1. That is, dissociation from the target proteins may promote CHP1 degradation.

In this study, we found that CHP1 binding-defective mutants of NHE1 (4Q and 4R) caused a marked acidic shift in the pH_i dependence of Na^+/H^+ exchange activity and completely impaired ATP depletion-induced inhibition and cytoplasmic alkalinization in response to various stimuli. As we reported previously (*32*), not only mutation of the CHP1 binding region, but also deletions of different regions in the amino-terminus (subdomain I, amino acids 515−595) of the NHE1 cytoplasmic domain also markedly reduced pH_i sensitivity. Thus, subdomain I with bound CHP1 appears to be a key structure that permits the putative "pH-sensor" to maintain a physiologically relevant conformation.

We found that mutation of EF3 or EF4 in CHP1 significantly reduced the Na^+/H^+ exchange activity in the physiological neutral pH_i range and reduced the cytoplasmic alkalinization in response to various extracellular signals by decreasing the pH_i sensitivity of NHE1. Thus, mutation of each EF-hand in CHP1 somehow affects the pH_i-sensing of NHE1, although we could not evaluate the function of the double mutant CHP1 (EF34m) because of its weak interaction with NHE1. We found that EF3m, EF4m, and EF34m proteins migrated slowly on SDS−PAGE, suggesting that significant conformational changes of CHP1 occur upon mutation of each EF-hand. Such conformational changes appear to be due to removal of Ca^{2+} rather than the amino acid substitution itself, because incubation with EGTA resulted in similar slow migration of the wild-type CHP1 on SDS−PAGE (data not shown). Thus, the bound Ca^{2+} may play an important role in maintaining the CHP1 structure, thereby preserving the physiological pH_i sensitivity of NHE1.

According to the structural model of CHP1 deduced from the three-dimensional structure of CaN-B (*43*), EF-hand Ca^{2+} binding motifs would be located on the surface opposite the side where CHP1 binds to NHE1. It is likely that the surface of CHP1 with tightly bound Ca^{2+} controls the pH_i-sensing by interacting with other region(s) of NHE1. We observed that the pH_i sensitivity of NHE1 was markedly reduced by insertion of one amino acid residue (alanine) just to the N-terminal side (position aa 504 or 508) of the CHP1 binding site of NHE1, while the CHP1 binding ability was preserved (our unpublished observations). Therefore, the correct spatial orientation of CHP1 would be important for regulation of NHE. Recently, we reported that mutation of Arg^{440} in intracellular loop 5 (IL5), which connects transmembrane helices 10 and 11, markedly reduces the pH_i sensitivity of NHE1 (*44*). Thus, IL5 may interact with the CHP1 surface with tightly bound Ca^{2+}.

Many EF-hand Ca^{2+} binding proteins are known to regulate the functions of their target proteins in response to cytosolic Ca^{2+} mobilization. However, it is unlikely that CHP1 functions as such a Ca^{2+} sensor in the regulation of NHE1 because the affinity for Ca^{2+} (K_d = ~2 nM) for the CHP1/NHE1 complex differs substantially from the range of intracellular Ca^{2+} concentrations (0.1−10 μM). Instead, two EF-hand motifs of CHP1 together with tightly bound Ca^{2+} would serve as structurally important elements for preserving the normal function of NHE1, as discussed above. Such a structural role has also been suggested in the C-terminal EF-hand motifs in CaN-B (*42*) and in CaM (*41*). On the other hand, we reported previously that CaM interacts in a Ca^{2+}-dependent manner with the middle of the cytoplasmic domain of NHE1, which in the unstipulated state serves as an auto inhibitory domain decreasing the pH_i sensitivity of NHE1 (*14*, *15*). The interaction of NHE1 with CaM is strictly Ca^{2+}-dependent, although it is much weaker than that with CHP1 (*14*). Previously, we proposed that NHE1 may be activated by Ca^{2+}-dependent interaction of CaM in response to Ca^{2+}-mobilizing signals (*15*). Our previous (*14*, *15*) and several recent reports (*45*−*48*) reinforced the idea that CaM serves as an important regulatory protein in activation of NHE1 in response to hyperosmotic stress or Ca^{2+}-mobilizing agonists. NHE1 thus appears to be dually regulated by two Ca^{2+} binding proteins, CHP1 and CaM, similar to CaN-A. The former would preserve the physiological pH_i sensitivity of NHE1, whereas the latter would play a role in sensing cytosolic Ca^{2+}.

In summary, our current results suggest that the interaction of CHP1 with NHE1 is crucial for preserving the physiological pH_i sensitivity of NHE1 and that tightly bound Ca^{2+} serves as an important structural element that is required for this role. The significant effects of mutations in EF-hands on NHE1 regulation prompted us to generate a more efficient dominant negative mutant CHP1. In addition, the functional difference between CHP1 and CHP2, which we reported recently (*13*), provides important information for identification of the critical residues of CHP1. Further studies including analyses of the functions of mutated or chimerical CHP1 and determination of the crystal structure of CHP1/NHE1 complex are required to elucidate the molecular mechanism of CHP regulation of NHE1 and other NHE family members.

REFERENCES

1. Wakabayashi, S., Shigekawa, M., and Pouysségur, J. (1997) Molecular physiology of vertebrate Na^+/H^+ exchangers, *Physiol. Rev. 77*, 51−74.
2. Orlowski, J., and Grinstein, S. (1997) Na^+/H^+ exchangers of mammalian cells, *J. Biol. Chem. 272*, 22373−22376.
3. Counillon, L., and Pouysségur, J. (2000) The expanding family of eucaryotic Na^+/H^+ exchangers, *J. Biol. Chem. 275*, 1−4.
4. Sardet, C., Franchi, A., and Pouysségur, J. (1989) Molecular cloning, primary structure, and expression of the human growth factor-activatable Na^+/H^+ antiporter, *Cell 56*, 271−280.
5. Orlowski, J., Kandasamy, R. A., and Shull, G. E., (1992) Molecular cloning of putative members of the Na/H exchanger gene family, *J. Biol. Chem. 267*, 9331−9339.
6. Tsé, C.-M., Brant, S. R. Walker, M. S., Pouysségur, J., and Donowitz, M. (1992) Cloning and sequencing of a rabbit cDNA encoding and intestinal and kidney-specific Na^+/H^+ exchanger isoform (NHE-3), *J. Biol. Chem, 267*, 9340−9346.
7. Numata, M., Petrecca, K., Lake, N., and Orlowski, J. (1998) Identification of a mitochondrial Na^+/H^+ exchanger, *J. Biol. Chem. 273*, 6951−6959.
8. Numata, M., and Orlowski, J. (2001) Molecular cloning and characterization of a novel (Na^+, K^+)/H^+ exchanger localized to the *trans*-Golgi network, *J. Biol. Chem. 276*, 17387−17394.
9. Baird, N., Orlowski, J., Szabo, E. Z., Zaun, H. Schultheis, P. J., Menon, A. G., and Shull, G. (1999) Molecular cloning, genomic

organization, and functional expression of Na^+/H^+ exchanger isoform 5 (NHE5) from human brain, *J. Biol. Chem. 274*, 4377−4382.
10. Goyal, S., Vanden Heuvel, G., and Aronson, P. S. (2003) Renal expression of novel Na^+/H^+ exchanger isoform NHE8, *Am. J. Physiol. 284*, F467−473.
11. Lin, X., and Barber, D. L. (1996) A calcineurin homologous protein inhibits GTPase-stimulated Na−H exchange, *Proc. Natl. Acad. Sci. U.S.A. 93*, 12631−12636.
12. Pang, T., Su, X., Wakabayashi, S., and Shigekawa, M. (2001) Calcineurin homologous protein as an essential cofactor for Na^+/H^+ exchangers, *J. Biol. Chem. 276*, 17367−17372.
13. Pang, T., Wakabayashi, S., and Shigekawa, M. (2002) Expression of calcineuin B homologous protein 2 protects serum deprivaion-induced cell death by serum-independent activation of Na^+/H^+ exchanger, *J. Biol. Chem. 277*, 43771−43777.
14. Bertrand, B., Wakabayashi, S., Ikeda, T., Pouysségur, J., and Shigekawa, M. (1994) The Na^+/H^+ exchanger isoform 1 (NHE1) is a novel member of the calmodulin-binding proteins: Identification and characterization of calmodulin-binding sites, *J. Biol. Chem. 269*, 13703−13709.
15. Wakabayashi, S., Bertrand, B., Ikeda, T., Pouysségur, J., and Shigekawa, M. (1994) Mutation of calmodulin-binding site renders the Na^+/H^+ exchanger (NHE1) highly H^+-sensitive and Ca^{2+} regulation-defective, *J. Biol. Chem. 269*, 13710−13715.
16. Voyno-Yasenetskaya, T., Conklin, B. R., Gilbert, R. L., Hooley, R., Bourne, H. R., and Barber, D. L. (1994) G alpha 13 stimulates Na−H exchange, *J. Biol. Chem. 269*, 4721−4724.
17. Bianchini, L., L'Allemain, G., and Pouysségur, J. (1997) The p42/p44 Mitogen-activated protein kinase cascade is determinant in mediating activation of the Na^+/H^+ exchanger (NHE1 isoform) in response to growth factors, *J. Biol. Chem. 272*, 271−279.
18. Takahashi, E., Abe, J.-I., Gallis, B., Aebersold, R., Spring, D. J., Krebs, E. G., and Berk, B. C. (1999) $p90^{RSK}$ is a serum-stimulated Na^+/H^+ exchanger isoform-1 kinase. Regulatory phosphorylation of serine 703 of Na^+/H^+ exchanger isoform-1, *J. Biol. Chem. 274*, 20206−20214.
19. Lehoux, S., Abe, J. I., Florian, J. A., and Berk, B. C. (2001) 14-3-3 binding to Na^+/H^+ exchanger isoform-1 is associated with serum-dependent activation of Na^+/H^+ exchange, *J. Biol. Chem. 276*, 15794−15800.
20. Yan, W., Nehrke, K., Choi, J., and Barber, D. L. (2001) The Nck-interacting kinase (NIK) phosphorylates the Na^+-H^+ exchanger NHE1 and regulates NHE1 activation by platelet-derived growth factor, *J. Biol. Chem. 276*, 31349−31356.
21. Aharonovitz, O., Zaun, H. C., Balla, T., York, J. D., Orlowski, J., and Grinstein, S. (2000) Intracellular pH regulation by Na^+/H^+ exchange requires phosphatidylinositol 4,5-bisphosphate, *J. Cell Biol. 150*, 213−224.
22. Li, X., Alvarez, B., Casey, J. R., Reithmeier, R. A. F., and Fliegel, L. (2002) Carbionic anhydrase II binds to and enhances activity of the Na^+/H^+ exchanger, *J. Biol. Chem. 277*, 36085−36091.
23. Barroso, M. R., Bernd, K. K., DeWitt, N. D., Chang, A., Mills, K., and Sztul, E. S. (1996) A novel Ca^{2+}-binding protein, p22, is required for constitutive membrane traffic, *J. Biol. Chem. 271*, 10183−10187.
24. Lin, X., Sikkink, R. A., Rusnak, F., and Barber, D. L. (1999) Inhibition of calcineurin phosphatase activity by a calcineurin B homologous protein, *J. Biol. Chem. 274*, 36125−36131.
25. Timm, S., Titus, B., Bernd, K., and Barroso, M. (1999) The EF-hand Ca^{2+}-binding protein p22 associates with microtubules in an N-myristoylation-dependent manner, *Mol. Biol. Cell 10*, 3473−3488.
26. Matsumoto, M., Miyake, Y., Nagita, M., Inoue, H., Shitakubo, D., Takemoto, K., Ohtsuka, C., Murakami, H., Nakamura, N., and Kanazawa, H. (2001) A serine/threonine kinase which causes apoptosis-like cell death interacts with a calcineurin B-like protein capable of binding Na^+/H^+ exchanger, *J. Biochem. (Tokyo) 130*, 217−225.
27. Nakamura, N., Miyake, Y., Matsushita, M., Tanaka, S., Inoue, H., and Kanazawa, H. (2002) KIF1Bβ2, capable of interacting with CHP, is localized to synaptic vesicles, *J. Biochem. (Tokyo) 132*, 483−492.
28. Inoue, H., Nakamura, Y., Nagita, M., Takai, T., Masuda, M., Nakamura, N., and Kanazawa, H. (2003) Calcineurin homologous protein isoform 2 (CHP2), Na^+/H^+ exchangers-binding protein, is expressed in intestinal epithelium, *Biol. Pharm. Bull. 26* (2), 148−155.
29. Pouysségur, J., Sardet, C., Franchi, A., L'Allemain, G., and Paris, S. (1984) A specific mutation abolishing Na^+/H^+ antiport activity in hamster fibroblasts precludes growth at nertral and acidic pH, *Proc. Natl. Acad. Sci. U.S.A. 81*, 4833−4837.
30. Wakabayashi, S., Fafournoux, P., Sardet, C., and Pouysségur, J. (1992) The Na^+/H^+ antiporter cytoplasmic domain mediates growth factor signals and controls "H^+-sensing", *Proc. Natl. Acad. Sci. U.S.A. 89*, 2424−2428.
31. Wakabayashi, S., Ogurusu, T., and Shigekawa, M. (1986) Factors influencing calcium release from the ADP-sensitive phosphoenzyme intermediate of the sarcoplasmic reticulum ATPase, *J. Biol. Chem. 261*, 9762−9769.
32. Ikeda, T., Schmitt, B., Pouysségur, J., Wakabayashi, S., and Shigekawa, M. (1997) Identification of cytoplasmic subdomains that control pH-sensing of theNa^+/H^+ exchanger (NHE1): pH-maintenance, ATP-sensitive, and flexible loop domains, *J. Biochem. (Tokyo) 121*, 295−303.
33. Strynadka, N. C. J., and James, M. N. G. (1989) Crystal structures of the helix-loop-helix calcium-binding proteins, *Annu. Rev. Biochem. 58*, 951−998.
34. Yap, K. L., Ames, J. B., Swindells, M. B., and Ikura, M. (1999) Diversity of conformational states and changes within the EF-hand protein superfamily, *Proteins 37*, 499−507.
35. Szebenyi, D. M. E., Obendorf, S. K., and Moffat, K. (1981) Structure of vitamin D-dependent calcium-binding protein from bovine intestine, *Nature 294*, 327−332.
36. Stemmer, P. M., and Klee, C. B. (1994) Dual Calcium Ion Regulation of Calcineurin by Calmodulin and Calcineurin B, *Biochemistry 33*, 6859−6866.
37. Pauls, T. L., Durussel, I., Cox, J. A., Clark, I. D., Szabo, A. G., Gagne, S. M., Sykes, B. D., and Berchtold, M. W. (1993) Metal binding properties of recombinant rat parvalbumin wild-type and F102W mutant, *J. Biol. Chem. 268*, 20897−20903.
38. Gross, M. D., Gosnell, M., Tsarbopoulos, A., and Hunziker, W. (1993) A functional and degenerate pair of EF hands contains the very high affinity calcium-binding site of calbindin-D_{28K}, *J. Biol. Chem. 268*, 20917−20992.
39. Burgoyne, R. D., and Weiss, J. L. (2001) The neuronal calcium sensor family of Ca^{2+}-binding proteins, *Biochem. J. 353*, 1−12.
40. Olwin, B. B., Edelman, A. M., Krebs, E. G., and Storm, D. R. (1984) Quantitation of energy coupling between Ca^{2+}, calmodulin, skeletal muscle myosin light chain kinase, and kinase substrates, *J. Biol. Chem. 259*, 10949−10955.
41. Johnson, J. D., Snyder, C., Walsh, M., and Flynn, M. (1996) Effects of myosin light chain kinase and peptides on Ca^{2+} exchange with the N- and C-terminal Ca^{2+} binding sites of calmodulin, *J. Biol. Chem. 271*, 761−767.
42. Feng, B., and Stemmer, P. M. (1999) Interactions of calcineurin A, calcineurin B, and Ca^{2+}, *J. Biol. Chem. 38*, 12481−12489.
43. Kissinger, C. R., Parge, H. E., Knighton, D. R., Lewis, C. T., Pelletier, L. A., Tempczyk, A., Kalish, V. J., Tucker, K. D., Showalter, R. E., Moomaw, E. W., Gastinel, L. N., Habuka, N., Chen, X., Maldonado, F., Barker, J. E., Bacquet, R., and Villafranca, J. E. (1995) Crystal structures of human calcineurin and the human FKBP12−FK506-calcineurin complex, *Nature 378*, 641−644.
44. Wakabayashi, S., Hisamitsu, T., Pang, T., and Shigekawa, M. (2003) Mutations of Arg^{440} and Gly^{455}/Gly^{456} oppositely change pH sensing of Na^+/H^+ exchanger 1, *J. Biol. Chem. 278*, 11828−11835.
45. Garnovaskaya, M. N., Mukhin, Y. V., Vlasova, T. M., and Raymond, J. R. (2003) Hypertonicity activates Na^+/H^+ exchange through Janus kinase 2 and calmodulin, *J. Biol. Chem. 278*, 16908−16915.
46. Mukhin, Y. V., Vlasova, T., Jaffa, A. A., Collinsworth, G., Bell, J. L., Tholanikunnel, B. G., Petus, T., Fitzgibbon, W., Ploth, D. W., Raymond, J. R., and Garnovskaya, M. N. (2001) Bradykinin B_2 receptors activate Na^+/H^+ exchange in mIMCD-3 cells via Janus kinase 2 and Ca^{2+}/calmodulin, *J. Biol. Chem. 276*, 17339−17346.
47. Robertson, M. A., Woodside, M., Foskett, J. K., Orlowski, J., and Grinstein, S. (1997) Muscarinic agonists induce phosphorylation-independent activation of the NHE−1 isoform of the Na^+/H^+ antiporter in salivary acinar cells, *J. Biol. Chem. 272*, 287−294.
48. Moor, AN, Murtazina, R. and Fliegel, L. (2000) Calcium and osmotic regulation of the Na^+/H^+ exchanger in neonatal ventricular myocytes, *J. Mol. Cell. Cardiol. 32*, 925−936.

BI0360004

Available online at www.sciencedirect.com
SCIENCE DIRECT®
Life Sciences 74 (2004) 2505–2513
Life Sciences
www.elsevier.com/locate/lifescie

Involvement of the 3′-untranslated region of cyclooxygenase-2 gene in its post-transcriptional regulation through the glucocorticoid receptor

Takeo Nishimori[a,b], Hiroyasu Inoue[a,*], Yukio Hirata[b]

[a]*Department of Pharmacology, National Cardiovascular Center Research Institute, 5-7-1 Fujishiro-dai, Suita, Osaka 565-8565, Japan*
[b]*Department of Clinical and Molecular Endocrinology, Graduate School, Tokyo Medical and Dental University, 1-5-45 Yushima, Bunkyo, Tokyo 113-8549, Japan*

Received 25 August 2003; accepted 6 October 2003

Abstract

Functional roles of the 3′-untranslated region (3′-UTR) of the human Cyclooxygenase-2 (COX-2) gene were evaluated by transient transfection using luciferase (Luc) reporter vectors into bovine arterial endothelial cells (BAEC). Insertion of the 3′-UTR into the downstream of a Luc coding region resulted in decreased reporter activity (23%), although insertion into the upstream was no effect. The reporter activity of the downstream insertion but not the upstream insertion was induced by bacterial lipopolysaccharide (LPS). Moreover, LPS selectively stabilized COX-2 mRNA. Next, to evaluate the role of the 3′-UTR together with glucocorticoid receptor (GR), a GR-expression vector was cotransfected with the reporter vector of the downstream insertion of the 3′-UTR. As a result, the LPS-induced reporter activity was suppressed by dexamethasone in a dose-dependent manner. These data suggest that the 3′-UTR of the COX-2 gene is involved in not only the induction by LPS but also the suppression by DEX of COX-2 expression at the post-transcriptional level.

Keywords: Cyclooxygenase; mRNA stability; AUUUA motif; Post-transcriptional regulation; Dexamethasone

Introduction

Prostaglandin (PG) endoperoxide synthase (EC1.14.99.1) known as cyclooxygenase (COX) is the rate-limiting enzyme in the biosynthesis of prostaglandins and thromboxane (Smith et al., 1996;

* Corresponding author. Tel.: +81-6-6833-5012x2588; fax: +81-6-6872-8090.
E-mail address: inoue@ri.ncvc.go.jp (H. Inoue).

0024-3205/$ - see front matter © 2004 Elsevier Inc. All rights reserved.
doi:10.1016/j.lfs.2003.10.017

Herschman, 1996). There exist two distinct isozymes, COX-1 and COX-2 (Kosaka et al., 1994; Appleby et al., 1994). While COX-1 is constitutively expressed in most cells, the expression of COX-2 is low under basal condition and induced by inflammatory mediators such as bacterial lipopolysaccharide (LPS) and cytokines, suggesting that COX-2 plays a critical role in inflammation. However, growing lines of evidence indicate that expression of COX-2 is differently and strictly regulated in various cell types and plays key roles in tumorigenesis, development, and circulatory homeostasis (Vane et al., 1998; DuBois et al., 1998; Oshima et al., 1996; Lim et al., 1997). Importantly, nuclear receptors such as glucocorticoid receptor (GR) and PPARγ modulate COX-2 expression mediated through both their ligands and expression patterns (Inoue et al., 1999, 2000). Dexamethasone (DEX), a synthetic glucocorticoid with a potent anti-inflammatory property, suppresses COX-2 expression in macrophage-like differentiated U937 cells, but not in vascular endothelial cells. This cell type-specific regulation may be physiologically important because thromboxane A_2 produced by macrophages has the opposite effect of prostacyclin produced by vascular endothelial cells. We have reported that this different effect of DEX is due to the modulation of COX-2 promoter activity by GR (Inoue et al., 1999). However, involvement of GR in the post-transcriptional regulation of COX-2 gene remains to be elucidated.

Transcriptional regulation of the COX-1 and COX-2 genes has been reported in numerous cell types using luciferase reporter vectors containing the 5′-flanking region of these genes. In bovine arterial endothelial cells (BAEC), the human COX-2 gene (− 1432/+59) showed promoter activity induced by LPS and TPA, whereas the human COX-1 gene (− 1010/+69) showed constitutive promoter activity (Inoue et al., 1995). However, the promoter activity of the human COX-2 gene (− 1432/+59) was 15-fold higher than that of the COX-1 gene (− 1010/+69) in BAEC, which was in contrast to the result that the amount of intrinsic COX-1 mRNA was greater than that of COX-2 mRNA (Inoue et al., 1995). Interestingly, the entire 3′-UTR of the human COX-2 gene encoded by exon 10 contains 17 copies of Shaw-Kamen sequence (AUUUA), which is found in many immediate-early genes and have been shown to enhance mRNA degradation (Kosaka et al., 1994; Appleby et al., 1994). In fact, recent reports showed that the 3′-UTR is involved in regulated stabilization of COX-2 mRNA especially by inducers of COX-2 expression (Newton et al., 1998; Gou et al., 1998, Dean et al., 1999; Dixon et al., 2000). However, there is no direct evidence that 3′-UTR is involved in the DEX-mediated suppression of COX-2 gene. On the other hand, we have found that the COX-2 promoter region acquires its suppressive response to DEX by transfection of expression vector for the glucocorticoid receptor (GR) into BAEC since BAEC express no detectable levels of GR (Inoue et al., 1999). In this study, we investigated the relationship between the 3′-UTR of the COX-2 gene and the GR. We indicated that the 3′-UTR is involved in suppression of COX-2 expression by DEX mediated through GR at the post-transcriptional level.

Materials and methods

Cell culture and reagents

BAEC were grown in Dulbecco's modified Eagle medium (DMEM) supplemented with 10% fetal calf serum (Flow Laboratories, Irvine, Scotland), 50 μM 2-mercaptoethanol, 100 units/ml penicillin, and 100 μg/ml streptomycin sulfate in a humidified atmosphere of 5% CO2 in air. DEX and LPS (from

Escherichia coli serotype 055, B5) were obtained from Sigma (St. Louis, MO) and used at concentrations of 100 nM and 1 μg/ml, respectively.

RNA analysis

Total RNA was isolated using the acid guanidinium thiocyanate procedure. RNAs were then subjected to electrophoresis. The cDNA probes for COX-2 and glyceraldehyde-3-phosphate dehydrogenase (GAPDH) were described previously (Inoue et al., 1999). The levels of mRNA were calculated on the basis of hybridization signals by imaging analyzers Fujix BAS 2500.

Plasmid construction

pGV-C (pGL2-Control Vector), the luciferase vector under control of the constitutive SV40 promoter/enhancer and pRShGRα, an expression vector for the human GR (Giguíre et al., 1986) were described previously (Inoue et al., 1999). Fig. 1 shows pGV-C and its derived reporter vectors containing the 3′-UTR of human COX-2 gene. This fragment contains a part of the coding region (57 bp) and the full-length of the 3′-UTR, which contains 17 copies of the ATTTA motif followed by 3 copies of the polyadenylation signal (AATAAA), and was obtained from the human COX-2 genomic clone λhPESII95 (kindly supplied by Dr. T. Tanabe) as described previously (Inoue et al., 2002). A reporter vector pG-3UCOX2 will express luciferase mRNA under controls of the SV40 enhancer/promoter and of the 3′-UTR (Inoue et al., 2002). This same fragment was ligated into *Sma* I site of pGV-C, which is located in the upstream of the coding region, in a sense (pG-5F3UCOX-2) and anti-sense orientations (pG-5R3UCOX-2), respectively. These clones are used as controls to evaluate the role of the 3′-UTR as enhancer/silencer for the SV40 promoter. DNA sequencing of relevant regions confirmed all of the constructs.

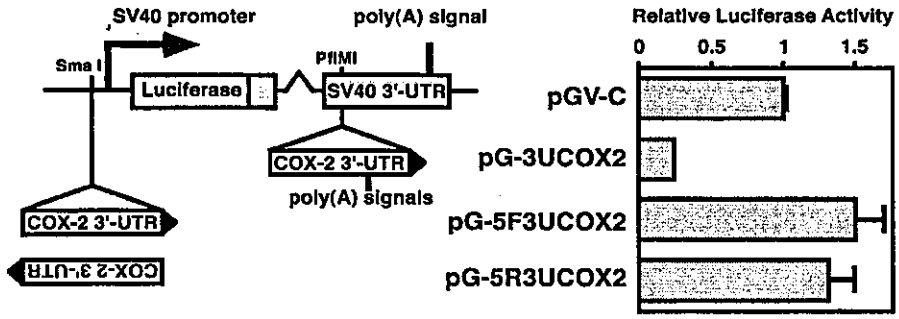

Fig. 1. Effect of the 3′-UTR of the human COX-2 on luciferase expression in a heterologous reporter system driven by SV40 promoter/enhancer. A 3′-UTR of the human COX-2 gene, which contains 17 copies of the AUUUA mRNA instability sequence and several polyadenylation signals, was inserted into pGV-C, a luciferase vector under control of the SV40 promoter/enhancer. A pG-3UCOX2 was constructed by insertion of the 3′-UTR into the downstream of a luciferase coding region in a sense orientation. pG-5F3UCOX2 and pG-5R3UCOX2 were constructed by insertion of the 3′-UTR into the upstream in a sense and anti-sense orientations, respectively. BAEC were transfected with each luciferase reporter together with pCMV-β-galactosidase control vector. Forty-eight hours after transfection, the cells were harvested, lysed and assayed for both luciferase and β-galactosidase activities. The results are presented as luciferase activities relative to the normalized luciferase activity of pGV-C. The data are presented as means ± standard deviations of three separate wells.

DNA transfections

Transfection of the reporter plasmids into BAEC was carried out as described previously (Inoue et al., 1999). Forty-eight hours after transfection using Trans IT™-LT-1 (Mirus), the cells were treated with LPS and/or DEX for 5 h. The cells were harvested, and their luciferase and β – galactosidase activities were determined by a luminometer (Berthold) and a method using chlorophenol red β-D-galactopyranoside as a substrate, respectively.

Results and discussion

The 3′-UTR of COX-2 destabilizes its mRNA, but does not suppress the transcriptional activity

The expression of COX-2 is tightly regulated at the levels of both post-transcription and transcription. To determine if the 3′-UTR of COX-2 mediates post-transcriptional regulation by changing mRNA stability and modulates the transcriptional activity, we examined the decay of chimeric luciferase cDNA constructs containing the 3′-UTR of COX-2 in three different positions. As shown in Fig. 1, transfection of pG-3UCOX2, a reporter vector containing the 3′-UTR at the downstream region of a luciferase coding region resulted in 23% reporter activity relative to that of pGV-C control vector in BAEC. On the other hand, pG-5F3UCOX2 and pG-5R3UCOX2, reporter vectors containing the 3′-UTR at the upstream region in a sense and anti-sense orientation, respectively, resulted in similar reporter activities with that of pGV-C. These results suggest that the 3′-UTR of COX-2 destabilizes its mRNA, but does not suppress the transcriptional activity. This destabilization of COX-2 mRNA by its 3′-UTR will explain the differences between higher COX-2 promoter activity and lower amount of COX-2 mRNA compared with those of COX-1 in BAEC (Inoue et al., 1995).

Transient stabilization of mRNA by LPS mediated through the 3′-UTR in BAEC

We have shown that LPS induces the COX-2 promoter activity in BAEC using luciferase reporter vectors of the human COX-2 gene (Inoue et al., 1995). Therefore, we next examined the involvement of the 3′-UTR of COX-2 in the induction of COX-2 mRNA by LPS. To eliminate the effect of the SV40 promoter activity of pG-3UCOX2, the luciferase activity of pG-3UCOX-2 was normalized by that of pGV-C since both reporter vectors used an identical SV40 promoter. As shown in Fig. 2A, normalized luciferase activity of pG-3UCOX2 maximally induced in 2.7 fold at 5 h and then returned in 1.8 fold at 7.5 h and 1.5 fold at 10 h after LPS treatment, respectively. On the other hand, treatment of LPS for 5 h did not induce the luciferase activity of pG-5F3UCOX2 or pG-5R3UCOX2 (data not shown). Next, to examine whether LPS attenuates the COX-2 mRNA instability, we chased the decay of COX-2 mRNA after the addition of actinomycin D, an inhibitor of transcription. As shown in Fig. 3, induced COX-2 mRNA by LPS for 4 h was almost completely degraded 2 h after the addition of actinomycin D in the absence of LPS. However, when the decay of COX-2 mRNA was significantly delayed in the presence of LPS. Taken together, these results indicates that LPS attenuates the mRNA instability mediated through the 3′-UTR of COX-2. Interestingly, the COX-2 promoter activity (– 327/ + 59) was maximally induced not at 5 h but at 7.5 h after LPS treatment (Fig. 2B), suggesting that the post-transcriptional regulation of COX-2 mRNA will has a different time-dependency of the transcriptional regulation of COX-2 gene.

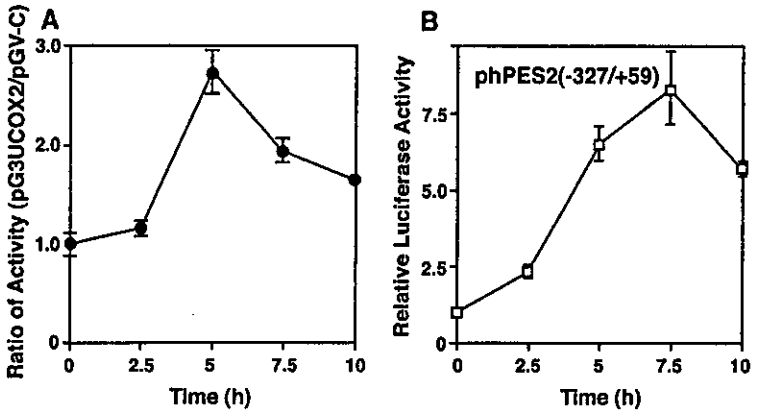

Fig. 2. Effect of LPS on the post-transcriptional control of the 3′-UTR of the human COX-2. BAEC were transfected with pGV-C, pG-3UCOX2 or phPES2(− 327/+59) together with pCMV-β-gal as an internal control for the transfection. Forty-eight hours after transfection, the cells were treated with or without LPS. At the indicated times, cells were harvested, lysed and assayed for both luciferase and β-galactosidase activities. The results are presented as ratio of luciferase activities of pG-3UCOX2 relative to that of pGV-C (A) or the luciferase activity of phPES2(− 327/+59) (B). The data are presented as means ± standard deviations of three separate wells. phPES2(− 327/+59) is a luciferase reporter vector driven by human COX-2 promoter region between −327 and +59 bp.

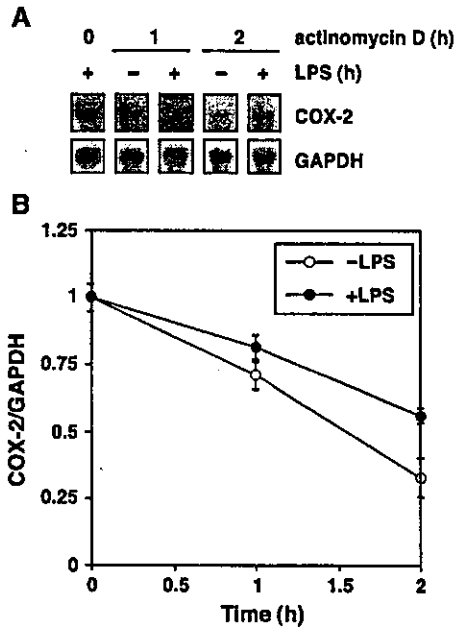

Fig. 3. Effect of LPS on COX-2 mRNA stability. BAEC were exposed to LPS (1 μg/ml) for 4 hours and then treated with actinomycin D (5 μg/ml) for a further 1 and 2 hours in the presence or absence of LPS. Extracted RNAs (10 μg/lane) were analyzed by RNA blot analysis (A). Expression levels of COX-2 mRNAs were normalized with amounts of GAPDH mRNA, and standardized to the value obtained at 4 hours of LPS-treatment. The data are presented as means ± standard deviations of three separate wells (B).

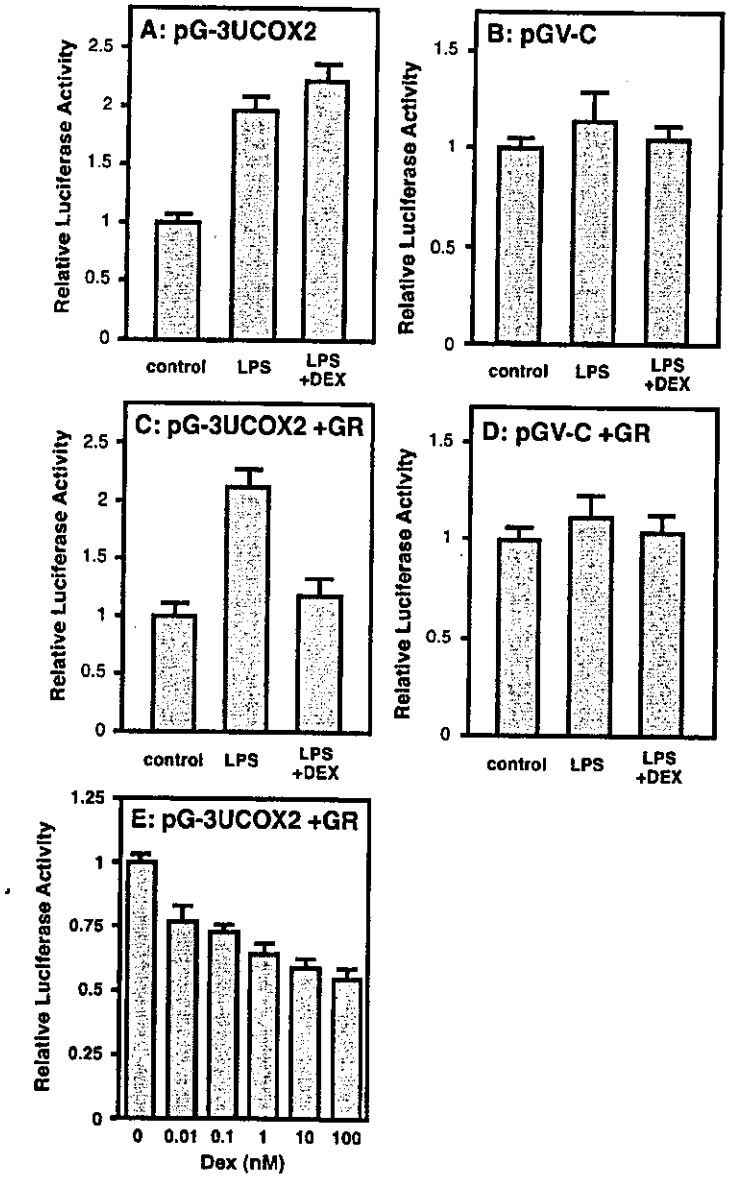

Fig. 4. Effect of DEX on the post-transcriptional control of the 3′-UTR of the human COX-2 in the presence or absence of GR. pG-3UCOX2 (0.3 μg) was transfected into BAEC without (A) or with pRShGRα (0.3 μg) (C), an expression vector for the GR, and with pCMV-βgal (0.05 μg) as an internal control for the transfection. For control experiments, pGV-C was used as a reporter vector instead of pG-3UCOX2 without (B) or with (D) pRShGRα. pGV-B, a promoterless reporter vector, was used instead of pRShGRα as a control and to maintain the total amount of plasmid equal (0.65 μg/well) for each transfection. Forty-eight hours after transfection, the cells were incubated for 5 h with or without 1 μg/ml LPS in the absence or presence of 100 nM DEX (A–D) or the indicated concentrations of DEX (E). The cells were then harvested, lysed and assayed for both luciferase and β-galactosidase activities. The results are presented as luciferase activities relative to the normalized luciferase activity in each control. The data are presented as means ± standard deviations of three separate wells.

DEX destabilizes the LPS-induced stabilization of mRNA by the 3′-UTR of COX-2 in the presence of the GR

To examine the effect of DEX on the 3′-UTR of COX-2, a reporter assay was performed using pG-3UCOX2 and pGV-C (Fig. 4A and B). In both cases, DEX did not suppress the reporter activity. This result is consistent with those reports by two groups (Newton et al., 1998; Gou et al., 1998), who concluded that the 3′-UTR of COX-2 is involved in the IL-1-induced stabilization of COX-2 mRNA, but not the DEX-induced down-regulation. However, we have found that DEX-mediated suppression of the promoter activity of the human COX-2 gene (−327/+59) is modulated by expression of the GR in BAEC (Inoue et al., 1999). Therefore, to examine the effect of DEX on the 3′-UTR in the presence of the GR, cotransfection of pRShGRα with the reporter vector pG-3UCOX2 into BAEC was performed. As shown in Fig. 4C, DEX suppressed the LPS-induced reporter activity in BAEC. On the other hand, even in the presence of the GR, DEX did not suppress the reporter activity in pGV-C (Fig. 4D), pG-5F3UCOX2 or pG-5R3UCOX-2 (data not shown). Moreover, the suppressive effect of DEX on the luciferase activity of pG-3UCOX-2 was dose-dependent (Fig. 4E). This dose-dependency is similar to that of the COX-2 promoter activity (−327/+59) in the presence of the GR (Inoue et al., 1999), indicating that the GR modulates the COX-2 expression at both the transcriptional and post-transcriptional levels.

DEX-mediated inhibition of COX-2 expression has previously been reported by several laboratories (Kujubu and Herschman, 1992; Xie et al., 1993; DeWitt and Meade, 1993; Masferrer et al., 1994; Crofford et al., 1994; Smith et al., 1996). This regulation occurs at both transcriptional and post-transcriptional levels. Concerning the transcriptional control, the NF-κB site (−223/−214) of the human COX-2 promoter region is involved in both the LPS-induced expression and its suppression by DEX in macrophage-like differentiated U937 cells (Inoue and Tanabe, 1998), and other cis-acting elements are also involved in BAEC transfected with the GR (Inoue et al., 1999). As for the post-transcriptional control, there are several reports indicating that DEX-mediated suppression of COX-2 mRNA occurs at the post-transcriptional level due to its destabilization (Newton et al., 1998; Xie et al., 1993; Ristimäki et al., 1996). Especially, the AUUUA sequence of the 3′-UTR was reported to be involved in the control of mRNA instability (Newton et al., 1998; Gou et al., 1998; Dean et al., 1999; Dixon et al., 2000). However, there has been no reports that the 3′-UTR is involved in the DEX-mediated suppression since DEX did not suppress the luciferase activity of pG-3UCOX2 (Fig. 4A) or similar constructs (Newton et al., 1998; Gou et al., 1998). This study demonstrates, for the first time, that the 3′-UTR is involved in the DEX-mediated suppression because of sufficient supply of the GR to the reporter system (Fig. 3C). Thus, this assay system will provide a suitable tool to analyze the molecular mechanism by which DEX interacts with the 3′-UTR to control the mRNA stability.

Acknowledgements

Authors wish to thank Dr. T. Tanabe for critical reading of the manuscript, and S. Bandoh, T. Sugimoto, and K. Sasagawa for their technical assistance. This work was supported in part by grants from the Ministry of Health and Welfare of Japan, the Ministry of Education, Science, Culture and Sports of Japan (a Grant-in-Aid for Scientific Research 11838021 and 13670110).

References

Appleby, S.B., Ristimäki, A., Neilson, K., Narko, K., Hla, T., 1994. Structure of the human cyclo-oxygenase-2 gene. Biochemical Journal 302 (Pt 3), 723–727.

Crofford, L.J., Wilder, R.L., Ristimäki, A., Sano, H., Remmers, E.F., Epps, H.R., Hla, T., 1994. Cyclooxygenase-1 and -2 expression in rheumatoid synovial tissues. Effects of interleukin-1 beta, phorbol ester, and corticosteroids. Journal of Clinical Investigation 93 (3), 1095–1101.

Dean, J.L., Brook, M., Clark, A.R., Saklatvala, J., 1999. p38 mitogen-activated protein kinase regulates cyclooxygenase-2 mRNA stability and transcription in lipopolysaccharide-treated human monocytes. Journal of Biological Chemistry 274 (1), 264–269.

DeWitt, D.L., Meade, E.A., 1993. Serum and glucocorticoid regulation of gene transcription and expression of the prostaglandin H synthase-1 and prostaglandin H synthase-2 isozymes. Archives of Biochemistry and Biophysics 306 (1), 94–102.

Dixon, D.A., Kaplan, C.D., McIntyre, T.M., Zimmerman, G.A., Prescott, S.M., 2000. Post-transcriptional control of cyclooxygenase-2 gene expression. The role of the 3′-untranslated region. Journal of Biological Chemistry 275 (16), 11750–11757.

DuBois, R.N., Abramson, S.B., Crofford, L., Gupta, R.A., Simon, L.S., Van De Putte, L.B., Lipsky, P.E., 1998. Cyclooxygenase in biology and disease. FASEB Journal 12 (12), 1063–1073.

Giguíre, V., Hollenberg, S.M., Rosenfeld, M.G., Evans, R.M., 1986. Functional domains of the human glucocorticoid receptor. Cell 46 (5), 645–652.

Gou, Q., Liu, C.H., Ben-Av, P., Hla, T., 1998. Dissociation of basal turnover and cytokine-induced transcript stabilization of the human cyclooxygenase-2 mRNA by mutagenesis of the 3′-untranslated region. Biochemical Biophysical Research Communications 242 (3), 508–512.

Herschman, H.R., 1996. Prostaglandin synthase 2. Biochimica et Biophysica Acta 1299 (1), 125–140.

Inoue, H., Yokoyama, C., Hara, S., Tone, Y., Tanabe, T., 1995. Transcriptional regulation of human prostaglandin-endoperoxide synthase-2 gene by lipopolysaccharide and phorbol ester in vascular endothelial cells. Involvement of both nuclear factor for interleukin-6 expression site and cAMP response element. Journal of Biological Chemistry 270 (42), 24965–24971.

Inoue, H., Tanabe, T., 1998. Transcriptional role of the nuclear factor κB site in the induction by lipopolysaccharide and suppression by dexamethasone of cyclooxygenase-2 in U937 cells. Biochemical Biophysical Research Communications 244 (1), 143–148.

Inoue, H., Umesono, K., Nishimori, T., Hirata, Y., Tanabe, T., 1999. Glucocorticoid-mediated suppression of the promoter activity of the cyclooxygenase-2 gene is modulated by expression of its receptor in vascular endothelial cells. Biochemical Biophysical Research Communications 254 (2), 292–298.

Inoue, H., Tanabe, T., Umesono, K., 2000. Feedback control of cyclooxygenase-2 expression through PPARγ. Journal of Biological Chemistry 275 (36), 28028–28032.

Inoue, H., Taba, Y., Miwa, Y., Yokota, C., Miyagi, M., Sasaguri, T., 2002. Transcriptional and posttranscriptional regulation of cyclooxygenase-2 expression by fluid shear stress in vascular endothelial cells. Arteriosclerosis, Thrombosis, and Vascular Biology 22 (9), 1415–1420.

Kosaka, T., Miyata, A., Ihara, H., Hara, S., Sugimoto, T., Takeda, O., Takahashi, E., Tanabe, T., 1994. Characterization of the human gene (PTGS2) encoding prostaglandin-endoperoxide synthase 2. European Journal of Biochemistry 221 (3), 889–897.

Kujubu, D.A., Herschman, H.R., 1992. Dexamethasone inhibits mitogen induction of the TIS10 prostaglandin synthase/cyclooxygenase gene. Journal of Biological Chemistry 267 (12), 7991–7994.

Lim, H., Paria, B.C., Das, S.K., Dinchuk, J.E., Langenbach, R., Trzaskos, J.M., Dey, S.K., 1997. Multiple female reproductive failures in cyclooxygenase 2-deficient mice. Cell 91 (2), 197–208.

Masferrer, J.L., Reddy, S.T., Zweifel, B.S., Seibert, K., Needleman, P., Gilbert, R.S., Herschman, H.R., 1994. In vivo glucocorticoids regulate cyclooxygenase-2 but not cyclooxygenase-1 in peritoneal macrophages. Journal of Pharmacology and Experimental Therapeutics 270 (3), 1340–1344.

Newton, R., Seybold, J., Kuitert, M.E., Barnes, P.J., 1998. Repression of cyclooxygenase-2 and prostaglandin E2 release by dexamethasone occurs by transcriptional and post-transcriptional mechanisms involving loss of polyadenylated mRNA. Journal of Biological Chemistry 273 (48), 32312–32321.

Oshima, M., Dinchuk, J.E., Kargman, S.L., Oshima, H., Hancock, B., Kwong, E., Trazakos, J.M., Evans, J.F., Taketo, M.M.,

1996. Suppression of intestinal polyposis in Apc delta716 knockout mice by inhibition of cyclooxygenase 2 (COX-2). Cell 87 (5), 803–809.

Ristimäki, A., Narko, K., Hla, T., 1996. Down-regulation of cytokine-induced cyclo-oxygenase-2 transcript isoforms by dexamethasone: evidence for post-transcriptional regulation. Biochemical Journal 318 (Pt 1), 325–331.

Smith, W.L., Garavito, R.M., DeWitt, D.L., 1996. Prostaglandin endoperoxide H synthases (cyclooxygenases)-1 and -2. Journal of Biological Chemistry 271 (52), 33157–33160.

Vane, J.R., Bakhle, Y.S., Botting, R.M., 1998. Cyclooxygenases 1 and 2. Annual Review of Pharmacology and Toxicology 38, 97–120.

Xie, W., Merrill, J.R., Bradshaw, W.S., Simmons, D.L., 1993. Structural determination and promoter analysis of the chicken mitogen-inducible prostaglandin G/H synthase gene and genetic mapping of the murine homolog. Archives of Biochemistry and Biophysics 300 (1), 247–252.

Characterisation of [^{123}I]iomazenil distribution in a rat model of focal cerebral ischaemia in relation to histopathological findings

Tomohito Kaji[1], Yuji Kuge[2], Chiaki Yokota[3], Masafumi Tagaya[5], Hiroyasu Inoue[4], Tohru Shiga[1], Kazuo Minematsu[6], Nagara Tamaki[1]

[1] Department of Nuclear Medicine, Hokkaido University Graduate School of Medicine, Kita-ku, Sapporo, Japan
[2] Department of Tracer Kinetics, Hokkaido University Graduate School of Medicine, Kita-ku, Sapporo, Japan
[3] Department of Pathogenesis, Research Institute, National Cardiovascular Center, Suita, Osaka, Japan
[4] Department of Pharmacology, Research Institute, National Cardiovascular Center, Suita, Osaka, Japan
[5] Department of Internal Medicine, National Osaka Hospital, Chuo-ku, Osaka, Japan
[6] Cerebrovascular Division, Department of Medicine, National Cardiovascular Center, Suita, Osaka, Japan

Received: 14 May 2003 / Accepted: 27 July 2003 / Published online: 8 October 2003

Abstract. Iodine-123 labelled iomazenil ([^{123}I]IMZ) has been reported to be a useful marker of neuronal viability. The brain distribution of [^{123}I]IMZ, however, has not been correlated with the pathophysiological response in detail after an ischaemic insult. To characterise [^{123}I]IMZ as a marker of neuronal viability, we compared its brain distribution with cyclooxygenase-2 (COX-2) expression, DNA fragmentation and cellular integrity. [^{123}I]IMZ and [^{125}I]IMP were injected into rats with focal cerebral ischaemia for the purpose of dual-tracer autoradiography. COX-2 and microtubule-associated protein-2 (MAP-2, a marker of cellular integrity) were immunostained. In situ DNA polymerase-I-dependent dUTP incorporation into damaged DNA was used as an indicator of DNA fragmentation. Lesion to normal ratios (LNRs) for [^{123}I]IMP and [^{125}I]IMZ were calculated. [^{123}I]IMZ accumulation was preserved in several regions with impaired [^{123}I]IMP accumulation. COX-2 expression was occasionally observed, whereas neither DNA fragmentation nor MAP-2 denaturation was detected in these regions. DNA fragmentation and impaired MAP-2 immunostaining were observed only in the regions with reduced LNRs for both tracers. The LNR for [^{123}I]IMZ was significantly lower in regions with impaired MAP-2 immunostaining (0.120±0.152, $P<0.0001$), in regions positive for dUTP incorporation (0.488±0.166, $P<0.0001$) and in regions positive for COX-2 expression (0.626±0.186, $P<0.001$) than in histologically normal regions (0.784±0.213). Thus, neuronal DNA is still intact and cellular integrity is maintained in the ischaemic regions with preserved [^{123}I]IMZ accumulation. The impairment of [^{123}I]IMZ accumulation precedes DNA fragmentation and denaturation of cellular integrity. These results provide the molecular basis of [^{123}I]IMZ distribution.

Keywords: [^{123}I]iomazenil – Cerebral ischaemia – Neuronal viability – Cyclooxygenase-2 – DNA fragmentation

Eur J Nucl Med Mol Imaging (2004) 31:64–70
DOI 10.1007/s00259-003-1319-6

Nagara Tamaki (✉)
Department of Nuclear Medicine,
Hokkaido University Graduate School of Medicine,
Kita 15 Nishi 7, 060-8638 Kita-ku, Sapporo, Japan
e-mail: natamaki@med.hokudai.ac.jp
Tel.: +81-11-7065150, Fax: +81-11-7067155

Introduction

An ischaemic stroke is one of the most common neuronal disorders, and the number of patients suffering from the disease is increasing. For the clinical evaluation of ischaemic stroke, it is very important to precisely detect the ischaemic penumbra, which is an ischaemically affected but still viable tissue, because the penumbral tissue can be salvaged by pharmacological and/or surgical interventions [1, 2, 3, 4].

Iodine-123 iomazenil ([^{123}I]IMZ) is a probe for central-type benzodiazepine receptor (BZR) for single-photon emission tomography (SPET). Since GABA receptors are abundant in the cortex and sensitive to ischaemic damage, specific radioligands to their subunits, the cerebral BZRs existing in GABA-A receptors, can be used as a marker of neuronal viability [5]. Thus, BZR imaging with [^{123}I]IMZ should be useful for detecting viable neurons, which may help detect the penumbra after an isch-